UNIVERSITY OF TROMSØ UIT

FACULTY OF SCIENCE AND TECHNOLOGY
DEPARTMENT OF CHEMISTRY

Theoretical studies of natural and magnetic circular dichroism

Harald Solheim

A dissertation for the degree of
Philosophiae Doctor

May 2011

Abstract

This dissertation presents theoretical studies mainly of natural and magnetic circular dichroism spectra. For magnetic circular dichroism, the importance of electron correlation effects, here included at the density-functional functional level of theory, and solvent effects are discussed, both being shown to have significant impact on the final spectra. In addition, a unified approach for calculating the temperate-independent contribution to MCD spectra are presented based on damped response theory. This approach is applicable also in energy regions with a high density of electronic states, where the calculation of MCD $\mathcal{B}$ terms based on residues of quadratic response functions may give unphysical results. It is argued for an abandonment of the conventional separation of the temperature-independent contribution into $\mathcal{A}$ and $\mathcal{B}$ terms since this separation may lead to incorrect analysis of the excited states.

For natural circular dichroism spectra, calculations have been performed both at the electronic level, as part of a study on Vitamin B_{12} including calculations of absorption and magnetic circular dichroism spectra, and at the vibronic level, in both cases employing density-functional theory. The study of vibrationally resolved circular dichroism was performed for a system where the observed spectrum is solely due to isotopic substitution. The model system, 2(*R*)-deutoriocyclopentanone, exists in two distinct, but near isoenergetic conformations with circular dichroism signals that nearly cancel each other, emphasizing a high requirement for computational accuracy.

The dissertation is concluded with a discussion on the construction of accurate model Hamiltonians for the simulation of vibronic spectra beyond the adiabatic approximation, using pyrazine as an example. Here, multireference wave-function based methods were employed in order to accurately describe potential energy surfaces over a large region of nuclear configuration space.

Acknowledgements

This dissertation is the result of a journey that started at the end of 2005. There has been a few ups and downs during the last few years, but the main impression is that it has been an exciting time and I am thankful for all the amazing people I had the opportunity to meet, work with, and learn from.

First of all I want to express my deep gratitude to Kenneth. It has been a privilege to be supervised by and learn from such an excellent scientist. I am certain that you will make a lasting impact on the scientific community here in Norway and to theoretical chemistry internationally. Even though you always had lots of other responsibilities, as the head of the chemistry department when I started out and later as the director of the Centre for Theoretical and Computational Chemistry, what amazes me is that you always found the time to answer emails or discuss things. Thanks for everything you have taught me about science, as well as the insights you shared about everything surrounding the actual disciplines.

Thanks to Marcel for welcoming me to visit his group in Waterloo for five months and for the great time I had there. Though in many ways different from Kenneth, you are really a true scientist. Whatever the subject, you always come up with insightful questions or comments. I hope you will continue to find the freedom to investigate the problems that stirs your curiosity. Ligou, thanks for the philosophical discussions over lunch. Your skills with knife and fork are just as bad as my skills with the chop sticks.

Na Lin, thanks for finally coming to Tromsø so we could work together like we had been talking about since the summer school in Sicily. Thanks for the nice food too! Thanks to Sonia, Patrick, Luca, Pawel, Karina, Xiao Zhao, Marcin, Attila, and Clemens who I had the pleasure of working with on the projects included in this dissertation.

Thanks to Lara, Andreas, Luca, Dmitry, and Jonas, who were there before the CTCC was established and who all still were around when I left for Bergen, at least in spirit. Adam, thanks for allowing the kids and me to watch your cat, and for the nice discus-

sions we had. Radovan, thanks for always being willing to help out with scientific or technical problems and whatever else. Thanks to all you guys at the CTCC for letting me win the 2010 World Cup bet and for the great farewell party. I really appreciate it! Maxime, Manu, Dan, Espen, Ying-Chan, Kathrin, Gosia, Arnfinn, and all the rest: It really wouldn't have been the same without you guys! The theoretical chemistry group was quite a bit smaller when I was studying for my master's degree so I know what I'm talking about.

Thanks to my parents and my sister, Inger, for stimulating my interest for science. I would also like to thank Karen and Helge for all the help watching the kids while I was busy writing up this dissertation.

Finally I want to express my heartfelt gratitude to my wonderful kids, Julie and Kristoffer, who help me remember what really is important in life, and to my beautiful wife, Line, who always have been patient and encouraging. Thanks for always being there with me throughout this journey.

Contents

Abstract I
Acknowledgements III
List of papers VII

1 Introduction **1**

2 Natural and magnetic circular dichroism **5**
2.1 Polarized light 5
2.2 The interaction Hamiltonian 7
2.3 Absorption 9
2.4 Natural circular dichroism 11
2.5 Magnetic circular dichroism 12

3 Quantum chemical methods **17**
3.1 Atomic units 17
3.2 The molecular Schrödinger equation 17
3.3 The vibrational wave function 19
3.3.1 Normal coordinates and normal modes 20
3.4 The electronic Schrödinger equation 21
3.5 Hartree–Fock theory 22
3.6 Correlated methods 24
3.7 Density functional theory 25
3.8 The polarizable continuum model 26

4 Response theory **29**
4.1 Response functions 29
4.2 Exact states 30

4.3 Approximate states 31
4.4 Absorption, CD, and MCD from response theory 33
4.5 Damped response theory 35
4.5.1 Molecular properties from damped response theory 37
4.6 Response theory for the polarizable continuum model 38

5 Vibronic models **41**
5.1 Adiabatic approximation 41
5.1.1 Analytical sum rules 43
5.1.2 Adiabatic Franck–Condon 44
5.1.3 Vertical gradient model 46
5.1.4 Vertical Franck–Condon 47
5.2 Vibronic model Hamiltonian 48
5.2.1 The diabatic basis 48
5.2.2 Diabatization scheme 49
5.2.3 The vibronic absorption and CD spectra 51

6 Summary of papers **53**
6.1 Solvent and correlation effects on the MCD $\mathcal{B}$ term 53
6.2 MCD $\mathcal{A}$ and $\mathcal{B}$ terms from damped response theory 54
6.3 Absorption, CD, and MCD of cobalamins 56
6.4 Isotopically engendered chirality 58
6.5 Systematic construction of vibronic coupling Hamiltonians 59

Bibliography **61**

List of papers

This dissertation is based on the following scientific papers:

I An IEF-PCM study of solvent effects on the Faraday B term of MCD
H. Solheim, L. Frediani, K. Ruud, and S. Coriani
Theor. Chem. Acc., **2008**, *119*, 231.

II Complex polarization propagator calculations of magnetic circular dichroism spectra
H. Solheim, K. Ruud, S. Coriani, and P. Norman
J. Chem. Phys., **2008**, *128*, 094103.

III The A and B terms of magnetic circular dichroism revisited
H. Solheim, K. Ruud, S. Coriani, and P. Norman
J. Phys. Chem A., **2008**, *112*, 9615.

IV Electronically excited states of Vitamin B_{12} and methylcobalamin: Theoretical analysis of absorption, CD and MCD data
H. Solheim, K. Kornobis, K. Ruud, and P. M. Kozlowski
J. Phys. Chem B., **2011**, *115*, 737.

V Vibrationally resolved circular dichroism spectra of a molecule with isotopically engendered chirality
N. Lin, H. Solheim, M. Nooijen, X. Zhao, K. Ruud, and M. Kwit
Manuscript.

VI On the systematic construction of vibronic coupling Hamiltonians: the interaction between the 1^1B_{3u} and 1^1B_{2u} states of pyrazine as an example
H. Solheim, A. Papp, C. Woywod, and K. Ruud
Manuscript.

Chapter 1

Introduction

The interaction between light and matter gives rise to physical phenomena that have intrigued humanity for thousands of years. An early example of this is the story of flood in the Hebrew Bible's book of Genesis, where the manifestation of the rainbow is described as a sign of a covenant between God and the human race. In the sami tradition, the northern lights, Aurora Borealis, likewise features a prominent role. As the story goes, a kind of troll known as stallu would come to get you if you forgot to whistle or wave to the northern lights. Even though modern science has provided us with a framework for understanding the physical origin of such phenomena, the colours surrounding us still fills us with wonder, from the rainbow and northern lights to the blue sky, red sunset, and variety of colors in a springtime field of flowers.

The scientific study of the physical origin of the rainbow started with Rene Descartes and Willebrord Snel in the early seventeenth century. They found that light would deviate from a straight path when passing through a raindrop, a process called refraction. Light of different colour, or wavelength, would have different deviation angles, causing a band of colours to be shown.

When light interacts with matter, light can be absorbed, emitted, or scattered. Refraction is an example of the latter, caused by the interference between forward scattered light and the unscattered component of the incident light. The study of absorption and emission of light gained momentum in the early nineteenth century with the observation that atoms will absorb and emit light with specific wavelengths; a finding that would lead up to the formulation of the theory of quantum mechanics a century later. Atoms have discreet states and can only absorb or emit quanta of energy corresponding to the differ-

ence between these states. The same holds for molecules, although here the description is complicated by the large difference in timescale betweeen the relative movements of electrons and the heavier nuclei, which means that transitions involving changes to the potential energy of electrons will require a lot more energy than transitions that only change the potential energy of the nuclei. Microwave and infrared light will typically cause transitions related the rotational and vibrational motion of the nuclei, respectively, while transitions involving changes to electronic energy levels are seen for visible and ultraviolet light. In this work, the interest will be in absorption of light in frequency regions corresponding to transitions between electronic energy levels.

Spectroscopy is the study of the interaction of electromagnetic radiation, or light, with matter. A special class of manifestations of this interaction is called optical activity, first observed in the form of optical rotation. Optical rotation is the phenomenon where the plane of polarization for a linearly polarized light beam is rotated when passing through an optically active medium. In absence of external static fields, it can be observed for molecules or crystal structures which a characteristic that called chirality, meaning handedness. Just like the left hand is not superimposable on the right hand, these molecules are not superimposable on their own mirror image.

The refractive index is closely related to absorption, which means that for chiral media the absorption is different for left and right circularly polarized light, a phenomenon called circular dichroism. Circular dichroism can be measured directly as the difference in absorption for left and right circularly polarized light, or as the ellipticity induced in a linearly polarized light beam, the former being prevalent today. It has a high sensitivity to the relative spatial arrangement of atoms within molecules, stereochemistry, and is therefore often used to analyse this, or as a fingerprinting tool for identifying molecules in a sample. In addition, it complements regular absorption spectroscopy since measuring intensity differences means that bands can be either positive or negative, making it easier to identify different transitions from these.

Optical rotation and circular dichroism in the absence of static external fields are two forms of natural optical activity, and can only be observed for chiral media. Optical rotation and circular dichroism can, however, be observed also for non-chiral media in the presence of an external static magnetic field. The perturbation by the static magnetic field gives rise to magnetic optical rotation, commonly called Faraday rotation or the Faraday effect, and magnetic circular dichroism. Like natural circular dichroism, magnetic circular dichroism provides information about the excited states of molecules

which is complementary to what is obtained from regular absorption spectroscopy. Magnetic circular dichroism is, however, applicable to all molecules, and can, in particular, provide information about degenerate or near-degenerate states, as will be seen in the following chapter.

Although combining experimental results from different spectroscopical techniques can provide a lot of information about the properties of a molecule, there will often be aspects of interest in that are not adequately understood from experiments alone. A valuable complement to experiments can then be provided by calculations based on molecular quantum-mechanical techniques. In theory-based calculations, microscopic properties of interest such as excitation energies and spectroscopic intensities can be obtained directly, elucidating the origin of spectral features observed.

Quantum mechanical expressions can only be evaluated exactly for a few simple systems such as the hydrogen atom, so for practical calculations on molecular systems, approximations need to introduced. Common approximations used in molecular quantum mechanics include separation of nuclear and electronic motion, as well as approximate treatment of the correlated motion of electrons and the effect of the environment surrounding the molecule of interest. These approximations will be discussed in relation to the various applications presented in this dissertation, which are mainly concerned with natural and magnetic circular dichroism.

The following chapter presents the properties related to natural and magnetic circular dichroism, as well as regular absorption spectroscopy. Chapter 3 then introduces the framework for describing the ground state of molecular systems, including the separation of electronic and nuclear motion. Treating only the electronic part of the problem, the theories used for calculating the response of these systems to electromagnetic radiation are presented in Chapter 4. In Chapter 5, the description of transitions involving both electronic and nuclear states, so-called vibronic transitions, will be discussed. Finally, a summary of the papers included in this dissertation and the main results obtained, are presented in Chapter 6.

Chapter 2

Natural and magnetic circular dichroism

This chapter presents the properties related to natural and magnetic circular dichroism, as well as regular absorption, using the semiclassical approximation. I will start with an introduction to polarized light in Sec. 2.1 and a presentation of the interaction Hamiltonian in Sec. 2.2. Then I will turn to a discussion of the spectroscopies of regular absorption and both natural and magnetic circular dichroism in Secs. 2.3–2.5.

2.1 Polarized light

The electric vector of a monochromatic linearly polarized electromagnetic wave may be given by [1, 2]

$$\mathbf{F}(\mathbf{r},t) = \mathbf{F}_0 \cos(\omega t - \kappa\cdot\mathbf{r}), \tag{2.1}$$

where ω is the frequency of the wave, $\mathbf{r}$ is the position vector. κ is the wave vector given by

$$\kappa = \frac{n\omega}{c_0}\mathbf{i}_z, \tag{2.2}$$

where n is the refractive index, c_0 is the speed of light, and $\mathbf{i}_z$ is unit vector in the direction of the propagation, which I have assumed to be the z direction.

The electric field can be reformulated as the real part of the following complex expression,

$$\tilde{\mathbf{F}}(\mathbf{r},t) = \tilde{\mathbf{F}}_0 e^{i(\kappa\cdot\mathbf{r}-\omega t)}, \tag{2.3}$$

which means that the electric field is given by

$$\begin{aligned}\mathbf{F}(\mathbf{r},t) &= \frac{1}{2}\left[\tilde{\mathbf{F}}_0 e^{i(\kappa\cdot\mathbf{r}-\omega t)} + (\tilde{\mathbf{F}}_0)^* e^{-i(\kappa\cdot\mathbf{r}-\omega t)}\right] \\ &= \frac{F_0}{2}\left[\mathbf{i}_F e^{i(\kappa\cdot\mathbf{r}-\omega t)} + \mathbf{i}_F^* e^{-i(\kappa\cdot\mathbf{r}-\omega t)}\right]. \end{aligned} \tag{2.4}$$

Here $\mathbf{i}_F$ is the unit vector for the electric vector of the polarized field.

Of particular importance for the later discussion of the interaction between electromagnetic fields and quantum mechanical systems is the vector potential. In the Coulomb gauge (see i.e. Ref. [1]), the vector potential $\mathbf{A}$ relates to respectively the electric and magnetic components of the field by

$$\mathbf{F} = -\frac{\partial \mathbf{A}}{\partial t} \tag{2.5}$$

$$\mathbf{B} = \nabla \times \mathbf{A}. \tag{2.6}$$

A vector potential consistent with Eq. 2.4 can then be given by

$$\mathbf{A}(\mathbf{r},t) = \frac{A_0}{2}\left[\mathbf{i}_F e^{i(\kappa\cdot\mathbf{r}-\omega t)} + \mathbf{i}_F^* e^{-i(\kappa\cdot\mathbf{r}-\omega t)}\right], \tag{2.7}$$

which means that

$$F_0 = -iA_0\omega \tag{2.8}$$

$$B_0 = -iA_0\frac{n\omega}{c_0}. \tag{2.9}$$

Note that the magnetic component of an electromagnetic field will be perpendicular to the electric component.

The linearly polarized wave discussed above is a special case of plane waves. Plane waves have the same value over any plane normal to the direction of propagation. These waves have no field components in the direction of propagation. This means that if the wave is propagating in the z direction, any plane wave can be written as a sum of two coherent waves linearly polarized in the x and y directions,

$$\tilde{\mathbf{F}} = \tilde{F}_x\mathbf{i}_x + \tilde{F}_y\mathbf{i}_y. \tag{2.10}$$

If the field components $\tilde{F}_x$ and $\tilde{F}_y$ have the same phase, $\tilde{\mathbf{F}}$ will be linearly polarized. Another special case occurs when $\tilde{F}_x$ and $\tilde{F}_y$ have equal magnitude and are $\pi/2$ out of phase. Then the polarization will be circular. In this case, the tip of the electric field

vector will, at a fixed point in space, describe a circle as time progresses. If the direction of rotation is clockwise when viewed against the direction of propagation, the circular polarization is said to be right-handed. This is because the tip of the electric field as a function of the direction of propagation z at a given time t then will form a right-handed helix. I will denote this case by a plus sign. The opposite polarization is said to be left-handed, and I will denote this by a minus sign. The two forms of circularly polarized light will then, in accordance with Eq. 2.4, be given by

$$\tilde{\mathbf{F}}_+((\mathbf{r},t) = \frac{F_0}{2}\left[\mathbf{i}_+ e^{i(\kappa\cdot\mathbf{r}-\omega t)} + \mathbf{i}_+^* e^{-i(\kappa\cdot\mathbf{r}-\omega t)}\right] \tag{2.11}$$

$$\tilde{\mathbf{F}}_-(\mathbf{r},t) = \frac{F_0}{2}\left[\mathbf{i}_- e^{i(\kappa\cdot\mathbf{r}-\omega t)} + \mathbf{i}_-^* e^{-i(\kappa\cdot\mathbf{r}-\omega t)}\right], \tag{2.12}$$

where the unit vectors for the electric field component of the two forms of circularly polarized light is

$$\mathbf{i}_+ = \frac{1}{\sqrt{2}}(\mathbf{i}_x + i\mathbf{i}_y) \tag{2.13}$$

$$\mathbf{i}_- = \frac{1}{\sqrt{2}}(\mathbf{i}_x - i\mathbf{i}_y). \tag{2.14}$$

2.2 The interaction Hamiltonian

The macroscopic absorption of light is closely related to microscopic properties of the sample studied. At the microscopic level, the behaviour of particles is described by quantum mechanics, where in the standard formulation, the information about the system is contained in a wave function $|\Psi(t)\rangle$. The time-evolution of this wave function is in the nonrelativistic domain given by the time-dependent Schrödinger equation,

$$\hat{H}(t)\,|\Psi(t)\rangle = i\hbar\frac{\partial\,|\Psi(t)\rangle}{\partial t}. \tag{2.15}$$

In this work, the microscopic system will be a molecule perturbed by static and dynamic electromagnetic fields. The semiclassical approximation will be employed, where the particles of the molecule is described with quantum mechanics, while the applied fields are described with classical electrodynamics. The Hamiltonian for the molecular system perturbed by external fields can then be given as

$$\hat{H}(t) = \hat{H}_0 + \hat{V}(t), \tag{2.16}$$

where $\hat{H}_0$ is the Hamiltonian for the system in absence of external fields, and $\hat{V}(t)$ describes the interaction of the system with the fields.

The Hamiltonian for the unperturbed system is given by

$$\hat{H}_0 = \hat{T}_{\text{el}} + \hat{T}_{\text{nuc}} + \hat{U}, \tag{2.17}$$

where $\hat{T}_{\text{el}}$ is the kinetic energy operator for the electrons, $\hat{T}_{\text{nuc}}$ the kinetic energy operator for the nuclei, and $\hat{U}$ the potential energy operator for the interaction between the particles. $\hat{H}_0$ describes a static system which will have well-defined energy levels. The quantum states $|n\rangle$ of the system and the corresponding energies E_n are respectively the eigenfunctions and eigenvalues of the time-independent Schrödinger equation

$$\hat{H}_0 |n\rangle = E_n |n\rangle , \tag{2.18}$$

The state $|0\rangle$ with the lowest energy is called the ground state.

The interaction operator introduces the time-dependence in the Hamiltonian. Including only effects to first order in the field, the interaction operator is given by [2, 3]

$$\hat{V}(t) = \sum_i \frac{q_i}{m_i} \mathbf{A}(r_i, t) \cdot \hat{\mathbf{p}}_i, \tag{2.19}$$

where the sum runs over all particles in the system, q_i is the charge of a particle, and m_i its mass. The linear momentum operator is given by

$$\hat{\mathbf{p}}_i = -i\hbar\nabla_i. \tag{2.20}$$

The interaction operator may be reformulated in terms of fields of radiation interacting with molecular multipole moments, giving

$$\hat{V}(t) = -F_0(\mathbf{i}_F \cdot \hat{\mu}) - B_0(\mathbf{i}_B \cdot \hat{\mathbf{m}}) - \frac{\nabla F_0}{2}(\mathbf{i}_z \cdot \hat{\theta} \cdot \mathbf{i}_F) + \cdots \tag{2.21}$$

where $\hat{\mu}$ is the electric dipole moment operator, $\hat{\theta}$ the electric quadrupole operator, and $\hat{\mathbf{m}}$ the magnetic dipole operator. These operators are defined respectively by

$$\hat{\mu} = \sum_i q_i \mathbf{r}_i \tag{2.22}$$

$$\hat{\mathbf{m}} = \sum_i \frac{q_i}{2m_i} (\mathbf{r}_i \times \mathbf{p}_i) \tag{2.23}$$

$$\hat{\theta} = \sum_i q_i \mathbf{r}_i \mathbf{r}_i, \tag{2.24}$$

where q_i, $\mathbf{r}_i$, and $\mathbf{p}_i$ are respectively the charge, position, and momentum of particle i, and I have used the traced form of the quadrupole operator.

Note that the unit vector in the direction of the magnetic component of the field is given by $\mathbf{i}_B = \mathbf{i}_z \times \mathbf{i}_F$.

2.3 Absorption

When the frequency of incident light matches the energy difference between two quantum states of the molecular system, the molecule may absorb light. The one-photon transition rate from an initial state $|i\rangle$ to a final state $|j\rangle$ is according to Fermi's golden rule proportional to the square of the transition moment of the perturbing operator as described in Refs. [4, 5, 3]

$$P_{ij}(\omega) = \frac{\pi}{2\hbar^2} \left|V_{ij}\right|^2 \delta(\omega - \omega_{ij}), \tag{2.25}$$

where ω is the frequency of the field, $\hbar\omega_{ij} = E_j - E_i$, and $V_{ij} = \left\langle i \left| \hat{V}(t) \right| j \right\rangle$. The Dirac delta function here ensures that the transition only occurs when the photon energy exactly matches the energy difference between the initial and the final state. Usually the initial state will be the ground state.

In spectroscopic conditions, the energies of the states will be broadened by several processes, like collisions among molecules and spontaneous emission of light. These processes are not easily included in the Hamiltonian and are therefore usually accounted for by replacing the delta function by a phenomenological lineshape function $g_{ij}(w)$ centered at ω_{ij}.

The spontaneous emission of light causes an exponential decay of the excited states. This effect may be described by making the energy of the excited state complex, as is done explicitly in Sec. 4.5, which causes resonance with an excited state to be obtained for a range of frequencies [2]. If only the spontaneous emission of light is considered, or this process dominates the broadening, the broadening function will be a Lorentzian function

$$g_{ij}(\omega) = \frac{1}{\pi} \frac{\Gamma}{(\omega - \omega_{ij})^2 + \Gamma^2}, \tag{2.26}$$

where Γ is the broadening parameter, here related to the inverse lifetime of the excited state. This process is called homogeneous broadening.

In experimental conditions, this picture is complicated by other processes contributing to the broadening. Collisions among molecules have already been mentioned, and are of course particularly important in the condensed phase. This is one example of the effect of the environment on the lineshape broadening. Another type of contribution comes from the Doppler effect, which is due to the effect of the molecular velocities on the excitation energies. Both these types of processes give rise to inhomogeneous broadening, which can be described by a Gaussian function

$$g_{ij}(\omega) = \frac{1}{\Gamma\sqrt{2\pi}} e^{\frac{(\omega-\omega_{ij})^2}{2\Gamma^2}}. \tag{2.27}$$

The absorption of light is according to the Beer-Lambert law proportional to both the light path length through the sample and the concentration of the sample. The absorption of light at a particular frequency may therefore be defined as

$$A = \varepsilon(\omega) C l, \tag{2.28}$$

where C is the concentration of the sample and l is the light path length through the sample. $\varepsilon(\omega)$ is called the molar decadic absorption coefficient and is the typical measure of absorption. Most commonly it is reported in units of l mol^{-1} cm^{-1}, and can then be identified as [6]

$$\varepsilon(\omega) = \frac{N_A \pi \omega}{1000 \times \ln(10) \times 2\hbar I_0} \sum_{ij} g_{ij}(\omega) \left|V_{ij}\right|^2, \tag{2.29}$$

where N_A is Avogadro's number and the quantities on the right-hand side of the equation are given in S.I. units. The summation runs over contributing transitions. The intensity of a monochromatic electromagnetic wave is given by

$$I_0 = \frac{n\varepsilon_0 c_0}{2} F_0^2 = \frac{\varepsilon_0 c_0^2}{2} F_0 B_0 = \frac{\varepsilon_0 c_0^3}{2n} B_0^2, \tag{2.30}$$

where n is the refractive index, c_0 the speed of light in vacuo, and ε_0 the vacuum permittivity.

The dominant contribution from the interaction operator in Eq. 2.21 to the absorption is from the dipole moment operator, and other terms like contributions from the electric quadrupole and magnetic dipole operators may therefore be neglected for the total absorption. For a sample of randomly oriented molecules, the molar decadic absorption coefficient is then from Eqs. 2.29 and 2.30 given as [3]

$$\varepsilon(\omega) = \frac{4\pi^2 N_A \omega}{3 \times 1000 \times \ln(10)(4\pi\varepsilon_0) n\hbar c_0} \sum_{ij} g_{ij}(\omega) \left|\mu_{ij}\right|^2, \tag{2.31}$$

where

$$\mu_{ij} = \sum_{\alpha=x,y,z} \langle i|\hat{\mu}_\alpha|j\rangle \tag{2.32}$$

is called the dipole transition moment between states i and j.

Often, the oscillator strength of a transition is used. This is a dimensionless quantity given by

$$f_{ij} = \frac{2m_e\omega_{ij}}{3\hbar e^2}\left|\mu_{ij}\right|^2, \tag{2.33}$$

where m_e and e is respectively the mass and charge of an electron.

2.4 Natural circular dichroism

In circular dichroism spectroscopy, the difference between the absorption of left and right circularly polarized light is measured. In analogy with regular absorption, it is conventionally reported as the difference in the molar decadic absorption coefficient,

$$\begin{aligned}\Delta\varepsilon(\omega) &= \varepsilon^{\mathrm{L}}(\omega) - \varepsilon^{\mathrm{R}}(\omega) &(2.34)\\ &= \frac{N_A\pi\omega}{1000\times\ln(10)\times 2\hbar I_0}\sum_{ij} g_{ij}(\omega)\left(\left|(V^L)_{ij}\right|^2 - \left|(V^R)_{ij}\right|^2\right), &(2.35)\end{aligned}$$

where superscripts L and R refer to left and right circularly polarized light respectively.

The difference in the square modulus of the interaction transition moment is, for circularly polarized light with the electric unit vectors defined by Eqs. 2.11–2.12, given by [2, 6]

$$\begin{aligned}\left|(V^L)_{ij}\right|^2 - \left|(V^R)_{ij}\right|^2 &= \frac{1}{2}\mathrm{Im}\left[(\mu_x)_{ij}(m_y)_{ij} + (\mu_y)_{ij}(m_x)_{ij}\right]F_0B_0\\ &\quad + \frac{i}{4}\mathbf{i}_z\cdot\left(\mu_{ij}\times\mu_{ji}\right)F_0^2 + \frac{i}{4}\mathbf{i}_z\cdot\left(\mathbf{m}_{ij}\times\mathbf{m}_{ji}\right)B_0^2, \qquad (2.36)\end{aligned}$$

where I have neglected the contributions from the quadrupole operator since these vanish when taking an orientational average. In the absence of external magnetic fields, the wave function may be taken to be real. In this case, we will have that $\mu_{ij} = \mu_{ji}$ and $\mathbf{m}_{ij} = \mathbf{m}_{ji}$, and the two last terms in Eq. 2.36 will therefore disappear for natural circular dichroism.

In the commonly used units of l mol^{-1} cm^{-1}, the difference in the molar decadic absorption coefficient will then for a sample of randomly oriented molecules be given

by [3]

$$\Delta\varepsilon(\omega) = \frac{16\pi^2 N_A \omega}{3 \times 1000 \times \ln(10)(4\pi\varepsilon_0)\hbar c_0^2} \sum_{ij} g_{ij}(\omega) R_{ij}, \tag{2.37}$$

where I have introduced the rotational strength

$$R_{ij} = \mathrm{Im}(\mu_{ij} \cdot \mathbf{m}_{ij}). \tag{2.38}$$

The rotational strength can only be nonzero for molecules with no improper rotation axes. This means that natural circular dichroism is only observed for chiral molecules.

2.5 Magnetic circular dichroism

Although natural optical activity is a feature only of chiral molecules, optical activity may be observed for all molecules in the presence of a static magnetic field with a component lying in the direction of the propagating light. In this case, the perturbing operator will have an extra term coming from the interaction with the static field. For a magnetic field applied in the direction of the propagating light, the perturbing operator then becomes

$$\hat{V}(t) = -F_0(\mathbf{i}_F \cdot \hat{\mu}) - B_0(\mathbf{i}_B \cdot \hat{\mathbf{m}}) - \frac{\nabla F_0}{2}(\mathbf{i}_z \cdot \hat{\theta} \cdot \mathbf{i}_F) - B_{\mathrm{ext}}(\mathbf{i}_z \cdot \hat{\mathbf{m}}) + \cdots, \tag{2.39}$$

where B_{ext} is the strength of the static magnetic field.

Expressions for MCD may be obtained by insertion of the interaction operator in Eq. 2.39 into the general expression for CD in Eq. 2.34. A more common approach, however, is to start with the expressions for CD in the absence of static magnetic fields and treat the interaction with the magnetic field as a perturbation to this system.

Looking now at Eq. 2.36, the first term will be zero for achiral systems. Moreover, it will not be affected by the static magnetic field to first order, so this term does not contribute to the MCD. Of the two remaining terms, the contribution from the latter will be negligible. Since the perturbed wave function can no longer be taken to be real, the terms involving $(\mu_{ij} \times \mu_{ij})$ and $(\mathbf{m}_{ij} \times \mathbf{m}_{ij})$ may contribute. The latter of these terms will have a dependence on the magnetic component of the dynamic field, causing it to be negligible compared to the former.

In addition to the transition moments, the external field will perturb the energies of the states. This will affect the lineshape of the transitions, and for a degenerate ground

state, the population of the degenerate components. The difference molar decadic coefficient can then be given as

$$\begin{aligned}\Delta\varepsilon(\omega) &= \frac{8\pi^2 N_A \omega}{3\times 1000\times \ln(10)(4\pi\varepsilon_0)\hbar c_0^2} \\ &\times \sum_{i_\alpha j_\beta} X_{i_\alpha}(B_{\rm ext}) \times g_{i_\alpha j_\beta}(\omega, B_{\rm ext}) \times i\left(\mathbf{i}_z \cdot \left[\mu_{i_\alpha j_\beta}(B_{\rm ext}) \times \mu_{j_\beta i_\alpha}(B_{\rm ext})\right]\right) \quad (2.40)\end{aligned}$$

where i_α and j_β refers to states in the degenerate manifold of states i and j respectively, and X_{i_α} is the Boltzmann weight of component i_α.

The static magnetic field will split the energies of degenerate states, an effect known as the Zeeman splitting. To first order in the field, the Boltzmann weight of a component of the degenerate manifold will be given by

$$X_{i_\alpha}(B_{\rm ext}) = \frac{1}{N_i}\left[1 + \frac{(\mathbf{i}_z \cdot \mathbf{m}_{i_\alpha i_\alpha})B_{\rm ext}}{kT}\right], \quad (2.41)$$

since the energy of this component is to first order in the field

$$\hbar\omega_{i_\alpha} = \hbar\omega_i - (\mathbf{i}_z \cdot \mathbf{m}_{i_\alpha i_\alpha})\, B_{\rm ext}. \quad (2.42)$$

In this approximation, it is assumed that the only effect the magnetic field has on the lineshape of an individual component of the degenerate manifold is to shift its energy. That is, it is assumed that the shape of the transition does not change. If the energy shift is negligible compared to the linewidth, the lineshape function may then be expanded in a Taylor series, which gives to first order in $B_{\rm ext}$,

$$g_{i_\alpha j_\beta}(\omega) \approx g_{ij}(\omega) + \frac{B_{\rm ext}}{\hbar}\frac{\partial g_{ij}}{\partial \omega}\left[(\mathbf{i}_z \cdot \mathbf{m}_{j_\beta j_\beta}) - (\mathbf{i}_z \cdot \mathbf{m}_{i_\alpha i_\alpha})\right]. \quad (2.43)$$

The wave functions will to first order in the field, be given by

$$|i(B_{\rm ext})\rangle = |i\rangle - \frac{B_{\rm ext}}{\hbar}\sum_{r\neq i}\frac{(\mathbf{i}_z \cdot \mathbf{m}_{ri})}{\omega_i - \omega_r}|r\rangle \quad (2.44)$$

$$\langle j(B_{\rm ext})| = \langle j| - \frac{B_{\rm ext}}{\hbar}\sum_{r\neq j}\frac{(\mathbf{i}_z \cdot \mathbf{m}_{jr})}{\omega_r - \omega_j}\langle r|, \quad (2.45)$$

which means that the perturbed dipole transition moments are, again to first order in $B_{\rm ext}$,

$$\mu_{i_\alpha j_\beta}(B_{\rm ext}) = \mu_{i_\alpha j_\beta} + B_{\rm ext}\left[\sum_{r\neq i}\frac{(\mathbf{i}_z \cdot \mathbf{m}_{i_\alpha r})}{\omega_r}\mu_{r j_\beta} + \sum_{r\neq j}\frac{(\mathbf{i}_z \cdot \mathbf{m}_{r j_\beta})}{\omega_r - \omega_i}\mu_{i_\alpha r}\right] \quad (2.46)$$

Inserting the expressions for the Boltzmann weights, the perturbed lineshape, and the perturbed dipole transition moments into Eq. 2.40, this gives [3]

$$\Delta\varepsilon(\omega) = -\frac{8\pi^2 N_A \omega}{3\times 1000\times \ln(10)(4\pi\varepsilon_0)\hbar c_0} B_{\text{ext}} \sum_{ij}\left\{ \frac{1}{\hbar}\frac{\partial g_{ij}(\omega)}{\partial\omega}\mathcal{A}_{ij} + g_{ij}(\omega)\left[\mathcal{B}_{ij} + \frac{\mathcal{C}_{ij}}{kT}\right]\right\}, \tag{2.47}$$

where the Faraday $\mathcal{A}$, $\mathcal{B}$, and $\mathcal{C}$ terms [7, 8, 9] are for a sample of oriented molecules given by

$$\mathcal{A}_{ij} = \frac{3i}{2N_i}\sum_{i_\alpha j_\beta}\left[(\mathbf{i}_z\cdot\mathbf{m}_{j_\beta j_\beta}) - (\mathbf{i}_z\cdot\mathbf{m}_{j_\beta j_\beta})\right]\left(\mathbf{i}_z\cdot\left[\mu_{i_\alpha j_\beta}\times\mu_{j_\beta i_\alpha}\right)\right] \tag{2.48}$$

$$\begin{aligned}\mathcal{B}_{ij} = \frac{3}{\hbar N_i}\sum_{i_\alpha j_\beta}\text{Im}\Bigg\{&\sum_{r\neq i}\frac{(\mathbf{i}_z\cdot\mathbf{m}_{ri_\alpha})}{\omega_r}\left(\mathbf{i}_z\cdot\left[\mu_{j_\beta r}\times\mu_{i_\alpha j_\beta}\right]\right)\\ &+\sum_{r\neq j}\frac{(\mathbf{i}_z\cdot\mathbf{m}_{j_\beta r})}{\omega_r-\omega_j}\left(\mathbf{i}_z\cdot\left[\mu_{ri_\alpha}\times\mu_{i_\alpha j_\beta}\right]\right)\Bigg\}\end{aligned} \tag{2.49}$$

$$\mathcal{C}_{ij} = \frac{3i}{2N_i}\sum_{i_\alpha j_\beta}(\mathbf{i}_z\cdot\mathbf{m}_{i_\alpha j_\alpha})\left(\mathbf{i}_z\cdot\left[\mu_{i_\alpha j_\beta}\times\mu_{j_\beta i_\alpha}\right)\right] \tag{2.50}$$

Since we are here interested in isotropic samples, an orientational average have to be performed. The final expressions for the Faraday $\mathcal{A}$, $\mathcal{B}$, and $\mathcal{C}$ terms then become

$$\mathcal{A}_{ij} = \frac{i}{2N_i}\sum_{i_\alpha j_\beta}\sum_{i'_\alpha j'_\beta}\left[\mathbf{m}_{j_\beta j'_\beta}\delta_{i_\alpha i'_\alpha} - \mathbf{m}_{i_\alpha i_\alpha}\delta_{j_\beta j'_\beta}\right]\cdot\left(\mu_{i'_\alpha j'_\beta}\times\mu_{j_\beta i_\alpha}\right) \tag{2.51}$$

$$\mathcal{B}_{ij} = \frac{1}{\hbar N_i}\sum_{i_\alpha j_\beta}\text{Im}\left\{\sum_{r\neq i}\frac{\mathbf{m}_{ri_\alpha}}{\omega_r}\cdot\left(\mu_{j_\beta r}\times\mu_{i_\alpha j_\beta}\right) + \sum_{r\neq j}\frac{\mathbf{m}_{j_\beta r}}{\omega_r-\omega_j}\cdot\left(\mu_{ri_\alpha}\times\mu_{i_\alpha j_\beta}\right)\right\} \tag{2.52}$$

$$\mathcal{C}_{ij} = \frac{i}{2N_i}\sum_{i_\alpha j_\beta}\sum_{i'_\alpha}\mathbf{m}_{i_\alpha i'_\alpha}\cdot\left(\mu_{i'_\alpha j_\beta}\times\mu_{j_\beta i_\alpha}\right). \tag{2.53}$$

The $\mathcal{A}$ and $\mathcal{C}$ terms can only be non-zero for systems with degenerate states since non-degenerate states can not have permanent magnetic moments. To have contributions from the temperature-dependent $\mathcal{C}$ term the ground state needs to be degenerate. Open-shell systems are the most typical examples of this, though also ground-state orbital degeneracies will give contributions to the $\mathcal{C}$ term.

The study of MCD will in the present work be restricted to systems showing only $\mathcal{A}$ and $\mathcal{B}$ terms. The $\mathcal{A}$ term is understood as being due to the splitting of degenerate states by the magnetic field, the so-called Zeeman effect. If the ground-state is non-degenerate

the $\mathcal{A}$ contribution from a degenerate excited state is proportional to its magnetic moment and may be used to provide a measure for this. The $\mathcal{A}$ has a characteristic derivative lineshape, which often makes it easy to identify in MCD spectra. As will be seen later, this is, however, not without pitfalls.

The $\mathcal{B}$ term is interpreted as a mixing of energy levels by the magnetic field. Since it does not depend on permanent magnetic moments, it may be observed for all molecular systems. The $\mathcal{B}$ contributions to MCD spectra have the shape of a broad absorption band with a positive or negative sign, similar to the contributions to natural CD spectra. Typically this term will have smaller intensities than the $\mathcal{A}$ term, so for systems with degenerate states, the $\mathcal{A}$ term contributions usually dominate.

A special case is represented by two near-degenerate states, where the $\mathcal{B}$ term for these states will then be dominated by the mixing of these two states, as can be seen by looking at the denominator in the second sum in Eq. 2.52. The two terms will have opposite sign, and relatively large intensities. Since the bands will be overlapping, this feature is not easily distinguished from an $\mathcal{A}$ term. The combined bands for the two near-degenerate states are therefore commonly referred to as a pseudo-$\mathcal{A}$ term.

Chapter 3

Quantum chemical methods

This chapter introduces the basic quantum mechanical methods used in this work. The time-independent molecular Schrödinger equation and the separation of electronic and nuclear motion in the Hamiltonian is first discussed. In Sec. 3.3, the vibrational part of the nuclear motion will be discussed, before the attention is turned to the solution of the electronic problem from Sec. 3.4 and onwards.

3.1 Atomic units

At the microscopic level, it is convenient to use atomic units, which is a unit system where the basic units are defined to be unity. These basic units are the electron mass m_e, the elementary charge e, the reduced Planck's constant $\hbar = h/2\pi$, and 4π times the permittivity of free space, $4\pi\varepsilon_0$. All microscopic properties will henceforth be given in atomic units when not stated otherwise. A more detailed introduction to this unit system can be found in standard text books on quantum chemistry, like Ref. [10].

3.2 The molecular Schrödinger equation

The time-independent molecular Schödinger equation may be written as

$$\hat{H}\,|\Psi(r,R)\rangle = \varepsilon\,|\Psi(r,R)\rangle\,, \tag{3.1}$$

where r and R represent respectively the electronic and nuclear coordinates, and ε is the molecular energy. $\hat{H}$ is the Hamiltonian operator for the system, which will be referred

to as the molecular Hamiltonian. Following Ref. [11], the molecular Hamiltonian may be written as

$$\hat{H} = \hat{T}_{\text{el}} + \hat{T}_{\text{nuc}} + \hat{U}(r,R), \tag{3.2}$$

where $\hat{T}_{\text{el}}$ is the kinetic energy operator for the electrons, $\hat{T}_{\text{nuc}}(R)$ the kinetic energy operator for the nuclei, and $\hat{U}(r,R)$ the interaction between the particles.

Due to the large difference in mass between the electrons and the nuclei, it is beneficial to treat the motion of these particles separately. We can then define the electronic Hamiltonian

$$\hat{H}_{\text{el}} = \hat{T}_{\text{el}} + \hat{U}(r,R), \tag{3.3}$$

which depends parametrically on the coordinates of the nuclei. $\hat{H}_{\text{el}}$ describes a system of fixed nuclei. Solving the corresponding electronic Schrödinger equation

$$\hat{H}_{\text{el}} \left|\Phi_n(r,R)\right\rangle = E_n(R) \left|\Phi_n(r,R)\right\rangle, \tag{3.4}$$

we get the adiabatic electronic states $|\Phi_n\rangle$ and the energies E_n of these states which depends parametrically on the nuclear positions. The full molecular wave function can then be expanded in the full set of electronic states

$$\left|\Psi(r,R)\right\rangle = \sum_n \left|\chi_n(R)\right\rangle \left|\Phi_n(r,R)\right\rangle, \tag{3.5}$$

where the expansion coefficients $|\chi_n(R)\rangle$ are referred to as nuclear wave functions.

Inserting this form of the wave function into Eq. 3.2 gives

$$(\hat{T}_{\text{nuc}} + E_n(R)) \left|\chi_n(R)\right\rangle - \sum_m \hat{\Lambda}_{nm} \left|\chi_m(R)\right\rangle = \varepsilon \left|\chi_n(R)\right\rangle, \tag{3.6}$$

where I have introduced nonadiabatic operators

$$\hat{\Lambda}_{nm} = \left\langle \Phi_n \,|\, \Phi_m \right\rangle \hat{T}_{\text{nuc}} - \left\langle \Phi_n \left| \hat{T}_{\text{nuc}} \right| \Phi_m \right\rangle \tag{3.7}$$

that couples electronic and nuclear motion. When the electronic states have a large energy separation, these coupling terms will be small. Neglecting the nonadiabatic operators, we get the Born-Oppenheimer adiabatic approximation, where the molecular wave function can be written as a product of a nuclear and electronic wave function

$$\left|\Psi(r,R)\right\rangle = \left|\chi_n(R)\right\rangle \left|\Phi_n(r,R)\right\rangle. \tag{3.8}$$

Neglecting the nonadiabatic operators is in most cases a good approximation, and it makes the computational problem a lot easier. The nonadiabatic operators will, however, often give sizable contributions when electronic states are close in energy. In particular, they show very complicated behaviour close to avoided crossings or conical intersections, where the adiabatic states change very fast with the nuclear coordinates.[11]

3.3 The vibrational wave function

If a given electronic state is energetically far apart from the other states, as for instance the electronic ground state usually is, it is safe to assume that the Born-Oppenheimer approximation can be invoked to describe this state. The nuclei can then be understood as moving on a potential surface obtained by solving Eq. 3.3 for all values of the nuclear coordinates R. The molecular Hamiltonian for an electronic state Φ_n can then be written as

$$\hat{H}_n(R) = \hat{T}_{\text{nuc}} + E_n(R). \tag{3.9}$$

The kinetic energy operator for the nuclei is given as

$$\hat{T}_{\text{nuc}} = -\frac{1}{2}\sum_{i}^{3N}\frac{\partial^2}{\partial q_i^2}, \tag{3.10}$$

where the summation runs over all nuclear coordinates and, following Wilson *et al.*,[12] mass-weighted Cartesian coordinates have been introduced as

$$q_i = \sqrt{M_i}R_i. \tag{3.11}$$

M_i and R_i are here respectively the mass and Cartesian coordinates of nuclei i.

The potential energy surface for the nuclei is described by the electronic energy, see Eq. 3.4, which unfortunately does not exist in a simple analytical form. The common solution is therefore to make a Taylor-expansion of the potential energy around the equilibrium geometry q_0, which gives

$$E_n(q) = E_n(q_0) + \frac{1}{2}\sum_{i,j=1}^{3N}\left(\frac{\partial^2 E_n}{\partial q_i \partial q_j}\right)_0 q_i q_j + \cdots, \tag{3.12}$$

since the gradient term disappears at this geometry. Keeping only terms up to second order in q, this is known as the harmonic approximation. For small displacements from the equilibrium geometry, this is often a reasonable approximation.

3.3.1 Normal coordinates and normal modes

The formulation of the potential energy in Eq. 3.12 is a bit cumbersome since it involves cross-terms between all nuclear coordinates. It is more convenient to use coordinates that diagonalize both $\hat{T}_{\text{nuc}}$ and E_n. These coordinates are known as normal coordinates, and can be defined as linear combinations of the mass-weighted Cartesian coordinates as follows

$$Q_k = \sum_{i=1}^{3N} l_{ki} q_i. \tag{3.13}$$

The molecular Hamiltonian in the harmonic approximation is now given as

$$\hat{H}_n(Q) = E_n(Q) + \sum_{k}^{3N} \left[-\frac{1}{2}\frac{\partial^2}{\partial Q_k^2} + \frac{1}{2}\left(\frac{\partial^2 E_n}{\partial Q_k^2}\right)_0 Q_k^2 \right], \tag{3.14}$$

which means that the problem can be solved for each of the $3N$ normal coordinates separately. The eigenvectors of the differential equations,

$$\left[-\frac{1}{2}\frac{\partial^2}{\partial Q_k^2} + \frac{1}{2}\left(\frac{\partial^2 E_n}{\partial Q_k^2}\right)_0 Q_k^2 \right] |\chi_{v_k,n}\rangle = \varepsilon_{v_k,n} |\chi_{v_k,n}\rangle, \tag{3.15}$$

are Hermite polynomials multiplied by a Gaussian function, and the eigenvalues are

$$\varepsilon_{v_k,n} = \left(v_k + \frac{1}{2}\right)\omega_k, \quad v_k = 0,1,2,\ldots, \tag{3.16}$$

where the frequencies ω_k are here given by

$$\omega_k = \left[\left(\frac{\partial^2 E_n}{\partial Q_k^2}\right)_0 \right]^{\frac{1}{2}}. \tag{3.17}$$

Unless the system is linear, the frequencies for 6 of these normal coordinates corresponding to the overall translation and rotation of the molecule will be zero. This kind of motion will not be treated here. The remaining $3N-6$ coordinates describe the vibrational motions of the nuclei, that is, the displacements of the nuclei relative to each other. For each of these normal coordinates, the nuclei move in phase, oscillating with the same frequency, but having different amplitudes. All nuclei will be at the equilibrium at the same time, and they will reach maximum displacement at the same time. Such a motion is called a normal mode of vibration.

The vibrational wave function for an electronic state Φ_n can then be written as a product of the wave functions for each normal coordinate

$$|\chi_n\rangle = \prod_{k=1}^{3N-6} |\chi_{v_k,n}\rangle\,, \tag{3.18}$$

and the molecular energy, disregarding translation and rotation, is given by

$$\varepsilon_n = E_n(Q_0) + \sum_{k=1}^{3N-6} \left(v_k + \frac{1}{2}\right) \omega_k, \tag{3.19}$$

where v_k is the vibrational quantum number or quanta of mode k.

3.4 The electronic Schrödinger equation

After having discussed the vibrational wave function, the focus will now shift to the solution of the electronic Schrödinger equation which provides the basis for most applications of quantum mechanics to problems related to chemistry. The focus here will be on Hartree–Fock and density functional theory (DFT). Although DFT has been used for most of the work presented here, Hartree–Fock theory will be presented first since this method is the starting point for many more advanced wave function based methods, and to show the similarities between this theory and DFT in the Kohn–Sham formalism. In the following I will use the second quantization formalism as presented in Ref. [13].

In the language of second quantization, the nonrelativistic spin-free electronic Hamiltonian can be written as

$$\hat{H}_{\mathrm{el}} = \hat{h} + \hat{g} + h_{\mathrm{nuc}}, \tag{3.20}$$

containing the one- and two-electron operators

$$\hat{h} = \sum_{pq} h_{pq} E_{pq} \tag{3.21}$$

$$\hat{g} = \sum_{pqrs} g_{pqrs} e_{pqrs}, \tag{3.22}$$

as well as the nuclear-nuclear repulsion term h_{nuc}.

Here I have introduced the one- and two-electron excitation operators that in terms of the creation and annihilation operators in second quantization are defined as

$$E_{pq} = \sum_{\sigma} a^{\dagger}_{p\sigma} a_{q\sigma} \tag{3.23}$$

$$e_{pqrs} = E_{pq}E_{rs} - \delta_{qr}E_{ps} = \sum_{\sigma\tau} a^{\dagger}_{p\sigma} a^{\dagger}_{r\tau} a_{s\tau} a_{q\sigma}, \tag{3.24}$$

where the summation over σ and τ runs over the two spin states of the electron, often referred to as the α and β spin. The excitation operators are multiplied by the one- and two-electron integrals

$$h_{pq} = \int \phi_p^*(\mathbf{r}) \left(-\frac{1}{2}\nabla^2 \right) \phi_q(\mathbf{r}) \, \mathrm{d}\mathbf{r} - \sum_K Z_K \int \frac{\Omega_{pq}(\mathbf{r})}{r_K} \, \mathrm{d}\mathbf{r} \tag{3.25}$$

$$g_{pqrs} = \iint \frac{\Omega_{pq}(\mathbf{r}_1)\Omega_{rs}(\mathbf{r}_2)}{r_{12}} \, \mathrm{d}\mathbf{r}_1 \, \mathrm{d}\mathbf{r}_2, \tag{3.26}$$

where ϕ are spin-orbitals, Z_K the charge of nuclei K, r_{12} the inter-electronic distance, and the overlap distributions is given by

$$\Omega_{pq}(\mathbf{r}) = \phi_p^*(\mathbf{r})\phi_q(\mathbf{r}). \tag{3.27}$$

3.5 Hartree–Fock theory

A common starting point in electronic structure theory is the Hartree–Fock (HF) method, in which the electronic wave function is represented by a single Slater determinant, or in the case of restricted HF theory in general, a single configuration state function (CSF). The CSF is a linear combination of Slater determinants that ensures that the wave function is an eigenstate of both the total and projected spins. In the following, I will only be concerned with closed-shell systems, and the CSF may then be written as a single determinant as follows

$$|0\rangle = \left(\prod_i a_{i\alpha}^\dagger a_{i\beta}^\dagger \right) |\mathrm{vac}\rangle \, , \tag{3.28}$$

where indices *i* refer to occupied orbitals, commonly referred to as inactive orbitals. The index *a* will refer to unoccupied orbitals, also called virtual orbitals.

The HF determinant may be parametrized by a unitary exponential orbital-rotation operator

$$\left|\tilde{0}(\kappa)\right\rangle = \exp(-\hat{\kappa}) \, |0\rangle \, , \tag{3.29}$$

where

$$\hat{\kappa} = \sum_{p>q} \kappa_{pq}(E_{pq} - E_{qp}) = \sum_{p>q} \kappa_{pq} E_{pq}^-. \tag{3.30}$$

Only rotations between occupied and virtual orbitals will affect the state $\left|\tilde{0}\right\rangle$. We can therefore restrict the summation to occupied-virtual orbital pairs

$$\hat{\kappa} = \sum_{ai} \kappa_{ai} E_{ai}^-. \tag{3.31}$$

The electronic energy is given by the expectation value of the Hamiltonian

$$E_0(\kappa) = \left\langle \tilde{0}(\kappa) \left| \hat{H}_{\mathrm{el}} \right| \tilde{0}(\kappa) \right\rangle . \tag{3.32}$$

Applying the variational principle, the HF state is defined by the rotation operator which minimizes the expectation value of the Hamiltonian, that is the state for which the expectation value is stationary

$$\delta E_0(\kappa) = \delta \left\langle \tilde{0}(\kappa) \left| \hat{H}_{\mathrm{el}} \right| \tilde{0}(\kappa) \right\rangle = 0. \tag{3.33}$$

Expanding the expectation value in terms of the orbital rotation operator, it is found that the conditions for the optimized HF state is

$$\left\langle \tilde{0}(\kappa) \left| [E_{ai}, \hat{H}_{\mathrm{el}}] \right| \tilde{0}(\kappa) \right\rangle = 0. \tag{3.34}$$

A single Slater determinant represents an electron which moves independently of the other electrons in the system. The HF state can therefore be obtained by finding the eigenfunctions of an effective one-electron operator, the Fock operator

$$\hat{f} = \sum_{pq} f_{pq} E_{pq}. \tag{3.35}$$

Applying the HF conditions in Eq. 3.34, and requiring that in the absence of two-electron interactions the Fock operator should reproduce the true Hamiltonian, the Fock operator becomes

$$f_{pq} = h_{pq} + \sum_i (2g_{pqii} - g_{piiq}). \tag{3.36}$$

The Hartree–Fock energy is then given by

$$E_0 = \sum_{pq} \tilde{D}_{pq} h_{pq} + \frac{1}{2} \sum_{pqrs} \tilde{d}_{pqrs} g_{pqrs} + h_{\mathrm{nuc}}, \tag{3.37}$$

where density matrices are defined as

$$\tilde{D}_{pq} = \left\langle \tilde{0} \left| E_{pq} \right| \tilde{0} \right\rangle \tag{3.38}$$

$$\tilde{d}_{pqrs} = \left\langle \tilde{0} \left| e_{pqrs} \right| \tilde{0} \right\rangle . \tag{3.39}$$

The one-electron density matrix can be chosen to be diagonal, and since for a closed-shell system only the elements with both indices inactive are nonzero, the energy can be given as

$$E_0 = 2 \sum_i h_{ii} + \sum_{ij} (2g_{iijj} - g_{ijji}) + h_{\mathrm{nuc}}. \tag{3.40}$$

3.6 Correlated methods

As mentioned above, in Hartree–Fock theory, an electron is described as moving independently of other electrons. An electron is then understood as moving in an effective potential set up by the nuclei and the other electrons in the system. In the real system, however, the interactions between the particles are instantaneous and will at any given time depend on their relative positions at this time. Considering the nuclei as fixed, we call the difference between this two descriptions for electron correlation. The correlation energy is then defined as the difference between the HF energy and the exact electronic energy of the system.

The exact wave function can be represented as a linear combination of all Slater determinants within a given basis. This is called the full configuration interaction (FCI) wave function

$$|\mathrm{FCI}\rangle = \sum_i C_i |i\rangle \,, \tag{3.41}$$

where C_i are the CI expansion coefficients and $|i\rangle$ are Slater determinants or, in general, CSF's. Computationally, this expression is only tractable for very small systems. It is therefore necessary to truncate the expansion in practical calculations.

In many cases, the FCI is dominated by a single reference configuration, the HF ground state. The electron correlation is then said to be "dynamic", and can be understood as a small, though important, perturbation of the uncorrelated system. Common methods to include dynamic correlation include truncated CI, coupled cluster (CC) theory, and Möller–Plesset (MP) perturbation theory.

For some systems, however, several configurations contribute significantly to the FCI wave function, and a single-reference configuration will not provide an adequate starting point for the treatment of dynamic correlation. This can be remedied by optimizing the expansion coefficients and the orbital coefficients simultaneously for the most important configurations, as is done in multiconfigurational self-consistent field (MCSCF) theory. The portion of the total electron correlation recovered by treating the multiconfigurational problem this way is typically called non-dynamical correlation. Various methods exist for using a multi-reference configuration as a starting point for treating dynamical correlation, including multi-reference CI and CC approaches and the perturbation theory based approaches CASPT2 [14, 15] and NEVPT2.[16]

3.7 Density functional theory

A computationally attractive alternative to treating electron correlation using wave function based methods is to use density functional theory. According to the Hohenberg–Kohn theorems,[17] the electronic energy can be expressed as a functional of the electron density ρ for a given external potential, and the density which minimizes the energy of the system in this external potential is the ground-state density.

The ground-state electronic energy can now be formulated as

$$E_0[\rho] = T[\rho] + V_{ee}[\rho] + V_{ne}[\rho], \tag{3.42}$$

where $T[\rho]$ is the kinetic energy, V_{ee} is the electron-electron interaction energy, and V_{ne} is the nuclear-electron interaction energy.

The problem with this approach is that the form of $T[\rho]$ and V_{ee} is unknown and these terms must therefore be approximated. The largest contribution to the energy of the system comes from the kinetic energy. However, for a system of noninteracting electrons the kinetic energy contribution can be calculated exactly. In the Kohn–Sham formalism, the energy is therefore instead solved for a fictitious system of noninteracting electrons having the same density as the real system, but moving in an effective external potential. The energy functional can then be reformulated as

$$E_0[\rho] = T_\mathrm{s}[\rho] + V^\mathrm{ext}[\rho] + J[\rho] + \mathrm{E_{xc}}[\rho] + h_\mathrm{nuc}, \tag{3.43}$$

where $T_\mathrm{s}[\rho]$ is the kinetic energy of the noninteracting system, $V^\mathrm{ext}[\rho]$ is the classical interaction of the electrons with the external potential, and $J[\rho]$ the classical Coloumb interaction of the density with itself. Solving for the effective external potential introduces the exchange-correlation functional which is unknown, but for which many approximations exist.

Since the wave function of a noninteracting system is a single Slater determinant, the density can in this formalism be expressed in terms of Slater determinants as

$$\rho(\mathbf{r}, \kappa) = \sum_{pq} \tilde{D}_{pq}(\kappa)\Omega_{pq}(\mathbf{r}), \tag{3.44}$$

where the overlap distribution Ω_{pq} is defined in Eq. 3.27 and the density matrix $\tilde{D}_{pq}$ in Eq. 3.38. Following Ref. [18], the Kohn-Sham energy can then be formulated in a

manner similar to the expression for the Hartree–Fock energy

$$E_0[\rho(\kappa)] = \sum_{pq} \tilde{D}_{pq}(\kappa) h_{pq} + \frac{1}{2} \sum_{pqrs} \tilde{D}_{pq}(\kappa) \tilde{D}_{rs}(\kappa) g_{pqrs} + \mathrm{E_{xc}}[\rho(\kappa)] + h_{\mathrm{nuc}}. \tag{3.45}$$

As mentioned above, the exchange-correlation functional $\mathrm{E_{xc}}$ needs to be approximated since the exact form of it is unknown. The simplest approximation would then be to let it only depend on the local density ρ. This is called the local density approximation (LDA)

$$\mathrm{E_{xc}^{LDA}}[\rho(\kappa)] = \int e_{\mathrm{xc}}(\rho(\mathbf{r},\kappa))\,\mathrm{d}\mathbf{r}, \tag{3.46}$$

which even though often useful for describing solid-state systems, is normally not a good approximation for molecular systems. A natural extension to this approach is to allow the functional to depend also on the gradient ζ of the electron density, which then gives the generalized gradient approximation (GGA)

$$\mathrm{E_{xc}^{GGA}}[\rho(\kappa)] = \int e_{\mathrm{xc}}(\rho(\mathbf{r},\kappa),\zeta(\mathbf{r},\kappa))\,\mathrm{d}\mathbf{r}. \tag{3.47}$$

Further improvent to the functional, in particular for molecular properties like atomization energies, bond lengths, and vibrational frequencies, can be made by incorporating some orbital exchange, also called exact exchange.[19, 20] A hybrid exchange-correlation functional can then be given as

$$\mathrm{E_{xc}^{hybrid}}[\rho(\kappa)] = \mathrm{E_{xc}^{GGA}}[\rho(\kappa)] - \frac{1}{2}\gamma \sum_{pqrs} \tilde{D}_{pq}(\kappa) \tilde{D}_{rq}(\kappa). \tag{3.48}$$

Analogous to the Fock-operator in Hartree–Fock theory, the Kohn–Sham states can be obtained as the eigenfunctions of the one-electron Kohn–Sham operator

$$F_{pq} = h_{pq} + \sum_i (g_{pqii} - \gamma g_{piiq}) + \int \left(\frac{\delta \mathrm{E_{xc}}}{\delta \rho} \right) \Omega_{pq}\,\mathrm{d}\mathbf{r}, \tag{3.49}$$

where γ of course is zero for LDA and GGA based methods.

3.8 The polarizable continuum model

So far I have assumed that the molecular system can be treated in isolation from the environment, which is a good assumption for molecules in the gas phase. Often, however, experimental studies are performed for molecules in solution where interaction with the

solvent may have a significant effect on the properties of the solute molecules. This interaction therefore needs to be included in the quantum mechanical system to give a good description of solvated molecules.

The solvent may be described by including discrete solvent molecules, as a continuum, or with a combination of these approaches. In this work, the interaction between the solute and the solvent will be described using the polarizable continuum model (PCM),[21, 22] where the solute molecule is placed in a cavity in a continuum describing the solvent. The continuum will be polarized by the solute, giving rise to apparent charges at the cavity surface.

In the integral equation formalism of PCM (IEF-PCM),[23, 24, 25] the interaction Hamiltonian is given as

$$\hat{H} = \hat{H}_{\mathrm{el}} + \hat{J} + \hat{Y} + \hat{X}(\tilde{0}) + U_{NN}, \tag{3.50}$$

where $\hat{J}$ is the interaction of the solute electrons with the apparent surface charges produced by the nuclei, $\hat{Y}$ the interactions of the solute nuclei with the apparent charges produced by the electrons, $\hat{X}(\tilde{0})$ the interaction of the electrons with the apparent charges produced by themselves, and U_{NN} the nuclear solvation energy.

In the second quantization formalism, these operators take the following form [26, 27]

$$\begin{aligned}
\hat{J} &= \hat{\mathbf{V}}^e \cdot \mathbf{q}^N = \sum_{\tau} \hat{V}^e_{\tau} q^N_{\tau} = \sum_{\tau,pq} \hat{V}_{\tau,pq} q^N_{pq} E_{pq} && (3.51)\\
\hat{Y} &= \mathbf{V}^N \cdot \hat{\mathbf{q}}^e = \sum_{\tau} V^N_{\tau} \hat{q}^e_{\tau} = \sum_{\tau,pq} V^N_{\tau} q^e_{\tau,pq} E_{pq} && (3.52)\\
\hat{X}(\tilde{0}) &= \hat{\mathbf{V}}^e \cdot \langle \tilde{0} | \hat{\mathbf{q}}^e | \tilde{0} \rangle = \sum_{\tau} \hat{V}^e_{\tau} \langle \tilde{0} | \hat{q}^e_{\tau} | \tilde{0} \rangle = \sum_{\tau,pqrs} V_{\tau,pq} E_{pq} q^e_{\tau,rs} D_{rs} && (3.53)\\
U_{NN} &= \mathbf{V}^N \cdot \mathbf{q}^N, && (3.54)
\end{aligned}$$

where the cavity surface is divided in small tesseras τ. $\hat{\mathbf{V}}^e$ and $\mathbf{V}^N$ are column vectors of electrostatic potentials produced by the solute electrons and nuclei respectively, and evaluated at the centers of these tesseras. Similarly, $\mathbf{q}_N$ collects the apparent surface charges produces by the nuclear charge density.

The wave function of the solute is obtained by minimizing the free energy of the solute

$$\delta G(\kappa) = \delta \langle \tilde{0}(\kappa) | \hat{G} | \tilde{0}(\kappa) \rangle = 0, \tag{3.55}$$

where since $\hat{J}$ and $\hat{Y}$ are formally equivalent [22], and U_{NN} does not affect the wave function, the free energy operator may be given as

$$\hat{G} = \hat{H}_0 + \hat{J} + \frac{1}{2}\hat{X}(\tilde{0}). \tag{3.56}$$

Chapter 4

Response theory

This chapter introduces the methodology employed to calculate the response of a molecular system to external electromagnetic fields. I will here restrict the discussion to the electronic problem, returning to the treatment of the full molecular Schrödinger equation and vibronic states in Chapter 5. The formalism used will mainly follow Refs. [3, 28, 29].

4.1 Response functions

The time-evolution of a state $|\psi(t)\rangle$ is given by the time-dependent Schrödinger equation

$$\hat{H}\,|\psi(t)\rangle = i\frac{\partial}{\partial t}\,|\psi(t)\rangle\,. \tag{4.1}$$

In the cases of interest here, the time dependence in the Hamiltonian is due to the interaction of the system with an external electromagnetic field that is assumed to be weak. This interaction can then be treated as a small perturbation to the time-independent Hamiltonian

$$\hat{H}(t) = \hat{H}_0 + \hat{V}(t). \tag{4.2}$$

In the frequency domain, the interaction operator may be written as

$$\hat{V}(t) = \int_{-\infty}^{\infty} \hat{V}^{\omega} e^{(-i\omega+\varepsilon)t} \mathrm{d}\omega, \tag{4.3}$$

where ε is a positive infitesimal ensuring that $\hat{V}(t)$ is zero before the external field is switched on at the time $t = -\infty$. If we only consider the electric dipole contribution, the interaction operator in Eq. 2.21 is given as

$$\hat{V}^{\omega} = -\hat{\mu}_{\alpha} F_{\alpha}^{\omega}, \tag{4.4}$$

where F_α^ω is a component of the electric field strength oscillating with frequency ω, and $\hat{V}^{-\omega} = (\hat{V}^\omega)^\dagger$ ensures that the perturbation is Hermitian. The Einstein notation of implicit summation over repeated indices will be used throughout this chapter.

Response functions can be defined from expanding the evolution of the expectation value of an operator $\hat{A}$ to various orders in the perturbation $\hat{V}(t)$,

$$\begin{aligned}\left\langle \psi(t) \left| \hat{A} \right| \psi(t) \right\rangle &= \left\langle 0 \left| \hat{A} \right| 0 \right\rangle + \int_{-\infty}^{\infty} \left\langle\left\langle \hat{A}; \hat{V}^{\omega_1} \right\rangle\right\rangle e^{-i\omega_1 t} e^{\varepsilon t} \mathrm{d}\omega_1 \\ &\quad + \int_{-\infty}^{\infty}\int_{-\infty}^{\infty} \left\langle\left\langle \hat{A}; \hat{V}^{\omega_1}, \hat{V}^{\omega_2} \right\rangle\right\rangle e^{-i(\omega_1+\omega_2)t} e^{2\varepsilon t} \mathrm{d}\omega_1 \mathrm{d}\omega_2 + \cdots . \end{aligned} \tag{4.5}$$

Molecular properties can be identified from these response functions and their residues [28]. For monochromatic perturbations, the integrals may be replaced by discrete sums over the relevant frequencies.

In the following, the Ehrenfest approach will be used to obtain expressions for the response functions as is done in Ref. [28]. It should be noted that in recent years the framework of quasienergy derivatives has gained increasing popularity.[30, 31] In addition to being more readily applicable to nonvariational wave functions than the Ehrenfest approach, this framework also has the advantage of an inherent symmetry with respect to exchange of operators. The picture provided by the Ehrenfest approach does, however, maintain a closer connection to the underlying physics involved, and I will therefore use this formalism below, noting that the same final expressions may be obtained in the framework of quasienergy derivatives.

4.2 Exact states

If the eigenstates and eigenvalues of the time-independent Schrödinger equation

$$H_0 \left| n \right\rangle = E_n \left| n \right\rangle \tag{4.6}$$

are known, these states may be used as a basis for expanding the time-dependent state $|\psi(t)\rangle$. One way of doing this is to define unitary rotation operators

$$\left| \psi(t) \right\rangle = e^{i\hat{P}(t)} \left| 0 \right\rangle , \tag{4.7}$$

where $\hat{P}(t)$ is a Hermitian operator given by

$$\hat{P}(t) = \sum_{n \neq 0} \left[P_n(t) \left| n \right\rangle \left\langle 0 \right| + P_n^*(t) \left| 0 \right\rangle \left\langle n \right| \right] . \tag{4.8}$$

The time-dependence of an expectation value is given by the Ehrenfest theorem.[32] For a general state-transfer operator $\hat{\Omega}_{nm} = |n\rangle\langle m|$ that has no explicit time dependence, this gives

$$\frac{\partial}{\partial t}\left\langle \psi(t)\left|\hat{\Omega}_{nm}\right|\psi(t)\right\rangle = -i\left\langle \psi(t)\left|[\hat{\Omega}_{nm},\hat{H}]\right|\psi(t)\right\rangle. \tag{4.9}$$

Expressions for the response functions in Eq. 4.5 are obtained by solving Eq. 4.9 to various orders in the perturbation.

In this work, we will focus on the linear and quadratic response functions. For exact states, the linear and quadratic response functions will be given by

$$\begin{aligned}\left\langle\left\langle \hat{A};\hat{V}^{\omega_1}\right\rangle\right\rangle &= \left\langle\left\langle \hat{A};\hat{B}\right\rangle\right\rangle_{\omega_1} \\ &= -\sum_{n\neq 0}\left[\frac{\left\langle 0\left|\hat{A}\right|n\right\rangle\left\langle n\left|\hat{B}\right|0\right\rangle}{\omega_n-\omega_1}+\frac{\left\langle 0\left|\hat{B}\right|n\right\rangle\left\langle n\left|\hat{A}\right|0\right\rangle}{\omega_n+\omega_1}\right] \qquad (4.10)\\ \left\langle\left\langle \hat{A};\hat{V}^{\omega_1},\hat{V}^{\omega_2}\right\rangle\right\rangle &= \left\langle\left\langle \hat{A};\hat{B},\hat{C}\right\rangle\right\rangle_{\omega_1,\omega_2} \\ &= \mathcal{P}_{-\sigma,1,2}\sum_{n,k\neq 0}\frac{\left\langle 0\left|\hat{A}\right|n\right\rangle\left\langle n\left|\hat{B}-\left\langle 0\left|\hat{B}\right|0\right\rangle\right|k\right\rangle\left\langle k\left|\hat{C}\right|0\right\rangle}{(\omega_n-\omega_\sigma)(\omega_k-\omega_2)}, \qquad (4.11)\end{aligned}$$

where $\omega_n = E_n - E_0$ and $\omega_\sigma = \omega_1+\omega_2$. $\mathcal{P}_{-\sigma,1,2}$ is a permutation operator that permutes the pairs of operators and frequencies $(\hat{A},-\omega_\sigma)$, $(\hat{B},\omega_1)$, and $(\hat{C},\omega_2)$, meaning that the quadratic response function consists of a total of 6 terms.

4.3 Approximate states

In practical calculations, the exact eigenstates of the time-independent Hamiltonian in Eq. 4.6 is not known. Instead of using a truncated set of approximate eigenstates as a basis for expanding the time-dependent wave-function, a different parametrization may be chosen. This choice of parametrization will then depend on the methodology used to obtain the time-independent reference state, which in most cases will be the ground state.

I will assume that the reference wave function is variationally optimized with respect to the energy of the system in the absence of external fields, and that a single-determinant approximation, that is Hartree–Fock or Kohn–Sham DFT, has been used. The time-dependent wave function can then be parametrized using a unitary orbital rotation operator as

$$|0(t)\rangle = e^{i\hat{\kappa}(t)}|0\rangle. \tag{4.12}$$

The Hermitian operator $\kappa(t)$ is defined as

$$\hat{\kappa}(t) = \sum_{ai} \left[\kappa_{ai}(t)\hat{a}_a^\dagger \hat{a}_i + \kappa_{ai}^*(t)\hat{a}_i^\dagger \hat{a}_a \right]. \tag{4.13}$$

where, as in Sec. 3.5, index i refers to inactive orbitals and a refers to virtual orbitals.

Following Norman *et al.*,[29] it is convenient to introduce a summation index n running over D pairs of indices (a,i). Letting $\hat{q}_n = \hat{a}_a^\dagger \hat{a}_i$, this gives

$$\hat{\kappa}(t) = \sum_{n=-D}^{D} \kappa_n \hat{q}_n, \tag{4.14}$$

where $n = 0$ is excluded from the summation, $\hat{q}_{-n} = \hat{q}_n^\dagger$, and $\kappa_{-n} = \kappa_n^*$.

Solving Eq. 4.9 to different orders in the perturbation, the linear and quadratic response functions may then be written as

$$\begin{aligned}
\left\langle\left\langle \hat{A}; \hat{V}^{\omega_1} \right\rangle\right\rangle &= \left\langle\left\langle \hat{A}; \hat{B} \right\rangle\right\rangle_{\omega_1} = -A_n^{[1]} N_n^B(\omega_1) && (4.15)\\
\left\langle\left\langle \hat{A}; \hat{V}^{\omega_1}, \hat{V}^{\omega_2} \right\rangle\right\rangle &= \left\langle\left\langle \hat{A}; \hat{B}, \hat{C} \right\rangle\right\rangle_{\omega_1,\omega_2} = [A_{nm}^{[2]} + A_{mn}^{[2]}] N_n^B(\omega_1) N_m^C(\omega_2) \\
&\quad + N_n^A(\omega_\sigma)[E_{nml}^{[3]} - \omega_1 S_{nml}^{[3]} + E_{nlm}^{[3]} - \omega_2 S_{nlm}^{[3]}] N_m^B N_l^C \\
&\quad + N_n^A(\omega_\sigma)[B_{nm}^{[2]} N_m^C(\omega_2) + C_{nm}^{[2]} N_m^B(\omega_1)], && (4.16)
\end{aligned}$$

where the response vectors solve the following set of linear response equations

$$\begin{aligned}
N_n^A(\omega_\sigma) &= A_l^{[1]} [E^{[2]} - \omega_\sigma S^{[2]}]_{ln}^{-1} && (4.17)\\
N_n^B(\omega_1) &= [E^{[2]} - \omega_1 S^{[2]}]_{nl}^{-1} B_l^{[1]} && (4.18)\\
N_n^C(\omega_2) &= [E^{[2]} - \omega_2 S^{[2]}]_{nl}^{-1} C_l^{[1]}. && (4.19)
\end{aligned}$$

The property, overlap, and Hessian matrices are in this parametrization given as

$$\begin{aligned}
A_n^{[1]} &= -\left\langle 0 \middle| \left[\hat{q}_n, \hat{A}\right] \middle| 0 \right\rangle && (4.20)\\
A_{nm}^{[2]} &= \frac{1}{2} \left\langle 0 \middle| \left[\hat{q}_n, \left[\hat{q}_m, \hat{A}\right]\right] \middle| 0 \right\rangle && (4.21)\\
S_{nl}^{[2]} &= \left\langle 0 \middle| \left[\hat{q}_n^\dagger, \hat{q}_l\right] \middle| 0 \right\rangle && (4.22)\\
S_{nlm}^{[3]} &= -\frac{1}{2} \left\langle 0 \middle| \left[\hat{q}_n^\dagger, [\hat{q}_m, \hat{q}_l]\right] \middle| 0 \right\rangle && (4.23)\\
E_{nl}^{[2]} &= -\left\langle 0 \middle| \left[\hat{q}_n^\dagger, [\hat{q}_l, \hat{H}_0]\right] \middle| 0 \right\rangle && (4.24)\\
E_{nlm}^{[3]} &= \frac{1}{2} \left\langle 0 \middle| \left[\hat{q}_n^\dagger, \left[\hat{q}_l, \left[\hat{q}_m, \hat{H}_0\right]\right]\right] \middle| 0 \right\rangle. && (4.25)
\end{aligned}$$

Constructing the inverses of $(E^{[2]} - \omega S^{[2]})$ for the linear response functions is not computationally tractable. Instead, the response equations in Eq. 4.17–4.19 are solved iteratively by multiplying $(E^{[2]} - \omega S^{[2]})$ with trial vectors N and comparing with the property gradient, i.e $A^{[1]}$, until convergence is obtained.[28] For a more detailed discussion of the form of the response equations for Kohn–Sham DFT, the reader is referred to Ref. [33].

4.4 Absorption, circular dichroism, and magnetic circular dichroism from response theory

For optical frequencies close to resonance with an electronic transition, the response functions will diverge, and the evaluation of the response functions themselves in these regions is therefore not particularly meaningful. Using linear response as an example, it is easily seen from the expression for exact states in Eq. 4.10 that this function will have poles at $\omega_1 = \pm \omega_n$. The residue of the response function gives transition moments

$$\lim_{\omega_1 \to \omega_n} (\omega_1 - \omega_n) \left\langle\left\langle \hat{A}; \hat{B} \right\rangle\right\rangle_{\omega_1} = - \left\langle 0 \left| \hat{A} \right| n \right\rangle \left\langle n \left| \hat{B} \right| 0 \right\rangle . \tag{4.26}$$

This means that the oscillator strength for absorption and the rotational strength for circular dichroism can be obtained from the residues of the appropriate linear response functions given in Eqs. 4.10 for exact states and in 4.15 for approximate states, with the positions of the poles determining the excitation energies. The oscillator strength is from Eq. 2.33 identified as

$$f_{0n} = \frac{2}{3\omega_n} S_n^{\alpha\alpha}, \tag{4.27}$$

where the dipole transition strength is given as

$$S^{\alpha\alpha} = - \lim_{\omega \to \omega_n} (\omega - \omega_n) \left\langle\left\langle \hat{\mu}_\alpha; \hat{\mu}_\alpha \right\rangle\right\rangle_\omega . \tag{4.28}$$

The rotational strength is similarly identified from Eq. 2.38 as

$$R_{0n} = - \lim_{\omega \to \omega_n} (\omega - \omega_n) \left\langle\left\langle \hat{\mu}_\alpha; \hat{m}_\alpha \right\rangle\right\rangle_\omega . \tag{4.29}$$

It should here be noted that although the rotational strength will be independent of the choice of gauge origin in the limit of a complete basis set, this is not generally the

case for calculations with finite basis sets. One approach to obtain gauge-origin independence also for finite basis set calculations is to use London orbitals, also known as Gauge-Including Atomic Orbitals.[34, 35] Another option is to use the velocity-gauge formalism for the dipole moment operator instead of the length-gauge formalism assumed above. In the velocity-gauge formalism, the rotational strength will always be gauge-origin independent, but its convergence with respect to basis set size is slower than in the length-gauge formalism.

The contributions to magnetic circular dichroism are commonly divided into three terms as discussed in Sec. 2.5. The term that has the closest analogy to natural circular dichroism is the Faraday $\mathcal{B}$ term. This term has often been calculated directly from the sum-over-states (SOS) expression in Eq. 2.52. Excitation energies and transition moments may then be obtained from poles and residues of linear response functions as shown in Eq. 4.26. The drawback of this approach is that a large number of states are often needed in the summation in order to get converged results.

An alternative approach, which has been used in this work, is to identify the $\mathcal{B}$ term from the single residue of a quadratic response function [36]

$$\mathcal{B}_{0n} = \varepsilon_{\alpha\beta\gamma}\mathrm{Im}\left(\lim_{\omega\to\omega_n}(\omega-\omega_n)\left\langle\left\langle\hat{\mu}_\alpha;\hat{\mu}_\beta,\hat{m}_\gamma\right\rangle\right\rangle_{\omega,0}\right). \tag{4.30}$$

As was the case for the rotational strength discussed above, the calculated $\mathcal{B}$ term will in general not be gauge-origin independent for finite basis set calculations. It should be noted that this residue includes some terms that are excluded from the expression for the $\mathcal{B}$ term in Eq. 2.52. This means that, depending on the symmetry of the system, the residue may have singularities causing unphysical divergencies for the calculated $\mathcal{B}$ terms. A suitable projection that removes these singularities is described in Ref. [37].

In the framework of quasienergy derivatives, a different approach for calculating the $\mathcal{B}$ term of MCD has been proposed.[38] The $\mathcal{B}$ term can here be identified from the magnetic-field derivative of the dipole transition strength in Eq. 4.28,

$$\mathcal{B}_{0n} = \frac{1}{2}\varepsilon_{\alpha\beta\gamma}\mathrm{Im}\left(\frac{\mathrm{d}S_n^{\alpha\beta}}{\mathrm{d}B_\gamma}\right)_{\mathbf{B}=0}. \tag{4.31}$$

This expression for the $\mathcal{B}$ term has the benefit of making it easier to include London atomic orbitals for gauge-origin independent calculations, in addition to being applicable to both variational and nonvariational wave functions.

The derivative approach may also be applied to the $\mathcal{A}$ term of MCD. The $\mathcal{A}$ term for a given degenerate state can be obtained from the magnetic-field derivative of its excitation energy [39]

$$\mathcal{A}_{0n} = \frac{1}{2}\varepsilon_{\alpha\beta\gamma}\sum_r \left[\left(\frac{\partial\omega_{n_r}}{\partial B_\gamma}\right)_{\mathbf{B}=0} \mathrm{Im}\left(S^{\alpha\beta}_{n_r}\right)\right], \tag{4.32}$$

where r runs over the degenerate states.

In this work, instead of calculating the $\mathcal{A}$ term directly, the attention has been turned to damped response theory, which in the Ehrenfest approach employed here also has been referred to as complex polarization propagator theory.[29] This approach, as will be discussed below, provides a unified framework for the $\mathcal{A}$ and $\mathcal{B}$ terms of MCD. It also avoids the problems with divergences due to near-degeneracies that might be encountered in some cases when calculating the $\mathcal{B}$ term as a residue. A drawback of the approach presented that should be noted, however, is that it is not as readily applicable to vibronic theory as the more conventional approaches employing the infinite lifetime approximation.

4.5 Damped response theory

In the formulation of response theory discussed above, the excited states are treated as having an infinite lifetime. This approximation is responsible for the divergence of the response functions close to resonance. Absorption spectra then become a progression of discrete poles. In reality, excited states will always decay to lower-lying states and will therefore have a finite lifetime. This is one of the effects that cause a broadening of the absorption bands. Typically this is simulated by multiplying the transition probabilities with a Lorentzian or Gaussian lineshape function as described in Sec. 2.3. Alternatively, the decay or relaxation of the excited states may be introduced in the equation of motion for the perturbed system, removing the singularities in the response function. This latter approach will here be referred to as damped response theory.[40]

Assuming that the system is in the ground state at thermal equilibrium, the Ehrenfest theorem may be modified to include decay of the excited states as follows [29]

$$\begin{aligned}\frac{\partial}{\partial t}\left\langle\psi(t)\left|\hat{\Omega}_{nm}\right|\psi(t)\right\rangle = \; & -i\left\langle\psi(t)\left|[\hat{\Omega}_{nm},\hat{H}]\right|\psi(t)\right\rangle - \gamma_{mn}\left[\left\langle\psi(t)\left|\hat{\Omega}_{mn}\right|\psi(t)\right\rangle\right. \\ & \left. - \left\langle\psi^{\mathrm{eq}}(t)\left|\hat{\Omega}_{mn}\right|\psi^{\mathrm{eq}}(t)\right\rangle\right],\end{aligned} \tag{4.33}$$

where γ_{mn} is the decay rate of state m to state n.

In the following, the excited states will be restricted to only relax directly to the ground state, and a common damping parameter, $\gamma = \gamma_{n0}$, for all excited states will be introduced. The damping parameter will in practical calculations be chosen to mimic the broadening of the experimental spectra. Since only the electronic part of the problem will be treated, this phenomenological parameter will also include the broadening of absorption bands due to the vibrational substructure of the electronic states.

For electronic states, it is normally safe to assume that the system is in the ground state at thermal equilibrium, and the last term in Eq. 4.33 can therefore be neglected. Restricting the equation of motion in this fashion is equivalent to introducing complex frequencies

$$\tilde{\omega} = \omega + i\gamma, \tag{4.34}$$

and solving the response functions in Sec. 4.3 for these complex frequencies.[40]

For the linear response function, the form of Eq. 4.15 will be retained in the damped formalism, with the modification that the response vector $N^B(\omega_1)$, and thus also the response function $\langle\langle \hat{A}; \hat{B} \rangle\rangle_{\omega_1}$, will be complex. The response vector

$$N_n^B(\omega_1) = [E^{[2]} - (\omega_1 + i\gamma)S^{[2]}]^{-1}_{nl} B_l^{[1]} \tag{4.35}$$

may then be separated into a real and an imaginary part as follows [41]

$$N^B(\omega) = N^{B,R}(\omega) + iN^{B,I}(\omega). \tag{4.36}$$

The real and imaginary parts of the response are then coupled through the damping parameter γ

$$[E^{[2]} - \omega S^{[2]}]N^{B,R} = B^{[1]} - \gamma S^{[2]} N^{B,I}(\omega) \tag{4.37}$$

$$[E^{[2]} - \omega S^{[2]}]N^{B,I} = \gamma S^{[2]} N^{R,I}(\omega). \tag{4.38}$$

Similarly, the expression for the quadratic response functions will be given by

$$\begin{aligned}\left\langle\left\langle \hat{A}; \hat{B}, \hat{C} \right\rangle\right\rangle_{\omega_1,\omega_2} =& [A_{nm}^{[2]} + A_{mn}^{[2]}] N_n^B(\omega_1) N_m^C(\omega_2) \\ &+ N_n^A(\omega_\sigma)[E_{nml}^{[3]} - (\omega_1 - i\gamma)S_{nml}^{[3]} + E_{nlm}^{[3]} - (\omega_2 - i\gamma)S_{nlm}^{[3]}] N_m^B N_l^C \\ &+ N_n^A(\omega_\sigma)[B_{nm}^{[2]} N_m^C(\omega_2) + C_{nm}^{[2]} N_m^B(\omega_1)].\end{aligned} \tag{4.39}$$

For real perturbations, the real part of the response functions is related to dispersion, that is polarizabilities and hyperpolarizabilites. The imaginary part may be shown to be

related to absorption.[41, 42] For odd numbers of imaginary perturbation operators, the relationship will be reversed.

4.5.1 Molecular properties from damped response theory

The identification of the contributions to absorption, CD, and MCD from the complex response functions can be made based on the refringent scattering approach presented in Ref. [1]. Assuming that the external field is oscillating with a single frequency, ω, the oscillating dipole moment can be expanded as

$$\begin{aligned}\mu_\alpha &= \mu^0_\alpha + \alpha_{\alpha\beta}F_\beta + \frac{1}{\omega}\alpha'_{\alpha\beta}\frac{\partial F_\beta}{\partial t} + \frac{1}{3}A_{\alpha,\beta\gamma}\frac{\partial F_{\beta\gamma}}{\partial t} + \frac{1}{3\omega}A'_{\alpha,\beta\gamma}\frac{\partial F_{\beta\gamma}}{\partial t} \\ &\quad + G_{\alpha\beta}B_\beta + \frac{1}{\omega}G'_{\alpha\beta}\frac{\partial B_\beta}{\partial t} + \cdots,\end{aligned} \tag{4.40}$$

where $F_{\alpha\beta} = \nabla_\alpha F_\beta$ is the electric field gradient. The tensors μ^0_α, $\alpha_{\alpha\beta}$ and so on are referred to as molecular property tensors and will be given by the appropriate response functions. In the framework of damped response theory, these property tensors will be complex, with the imaginary part being related to absorption when the perturbing operator is real.

The dominant contribution to regular absorption comes from the imaginary part of the electric dipole polarizability, identified as

$$\alpha_{\alpha\beta} = \langle\langle \hat{\mu}_\alpha; \hat{\mu}_\beta \rangle\rangle_\omega. \tag{4.41}$$

The mixed electric dipole-magnetic dipole polarizability $G'_{\alpha\beta}$, and the mixed electric dipole-electric quadrupole polarizability, $A_{\alpha,\beta\gamma}$, contributes to natural CD. Contributions from the latter will, however, cancel out for isotropic samples, so the main contributions surviving come from the real part of

$$G'_{\alpha\beta} = \langle\langle \hat{\mu}_\alpha; \hat{m}_\beta \rangle\rangle_\omega, \tag{4.42}$$

noting that one of the perturbing operators is imaginary. Both A and $G'_{\alpha\beta}$ vanishes for nonchiral systems.

Another contribution to CD comes from the response to first order in the time-derivative of the electric field, $\alpha'_{\alpha\beta}$, but this is only non-zero in the presence of an

external time-odd influence, such as a static magnetic field. This property tensor is responsible for MCD, and may be expanded in the static magnetic field as follows,

$$\alpha'_{\alpha\beta}(B) = \alpha'_{\alpha\beta}(0) + \alpha'^{(m)}_{\alpha\beta,\gamma} B_\gamma \cdots . \tag{4.43}$$

The response to first order in the magnetic field, $\alpha'^{(m)}_{\alpha\beta,\gamma}$, is responsible for the temperature-independent part of the MCD signal, which is usually interpreted in terms of the $\mathcal{A}$ and $\mathcal{B}$ terms discussed in Sec 2.5. In the damped response theory framework, they are identified from the real part of a single response function,

$$\alpha'^{(m)}_{\alpha\beta,\gamma} = \langle\langle \hat{\mu}_\alpha; \hat{\mu}_\beta, \hat{m}_\gamma \rangle\rangle_{\omega,0}, \tag{4.44}$$

again noting the presence of an imaginary perturbing operator.

4.6 Response theory for the polarizable continuum model

When a solvated system is perturbed by a dynamic field, both the dynamics of the solute and the solvent must be taken into account. In a fast process, the solvent will not be able to stay in equilibrium with the fast changes in the solute electron distribution. In the nonequilibrium formalism, this may be accounted for by partitioning the bielectronic term in Eq. 3.53 in a fast component $\hat{X}^d(\tilde{0})$ that always will be in equilibrium with the electron density of the solute, and a slow component $\hat{X}^{in}(\rho^{in})$ that is kept fixed to a frozen electron density ρ^{in}. The fast component may be related to the solvent electronic distribution close to the cavity which instantenously equilibrates to the new electron density of the solute, while the slow component is related to other degrees of freedom in the solvent [43, 44].

The free energy operator for the solvated system in a dynamic external field is now given by [27]

$$\hat{G} = \hat{H}_0 + \hat{J} + \hat{X}^{in}(\rho^{in}) + \frac{1}{2}\hat{X}^d(\tilde{0}) + \hat{V}(t). \tag{4.45}$$

Response equations for PCM can then be obtained by replacing the derivatives of the electronic energy $E^{[n]}$ in Eqs. 4.16–4.19 with the corresponding derivatives of the free energy of the solvated system $G^{[n]}$

$$G^{[2]}_{nl} = E^{[2]}_{nl} + \mathbf{V}^{[2]}_{nl} \cdot [\mathbf{q}^N + \mathbf{q}^{in} + \mathbf{q}^d] + \mathbf{V}^{[1]}_n \mathbf{q}^{d[1]}_l \tag{4.46}$$

$$G^{[3]}_{nlm} = E^{[3]}_{nlm} + \mathbf{V}^{[3]}_{nlm} \cdot [\mathbf{q}^N + \mathbf{q}^{in} + \mathbf{q}^d] + \mathbf{V}^{[2]}_{nl} \mathbf{q}^{d[1]}_m + \mathbf{V}^{[1]}_n \mathbf{q}^{d[2]}_{lm} . \tag{4.47}$$

$\mathbf{q}^N$ are here a column vector of apparent charges produced by solvent nuclei, $\mathbf{q}^{in}$ apparent charges produced by the frozen reference electron density ρ^{in}, and $\mathbf{q}^d$ apparent charges produced by the dynamic electron density.

Chapter 5

Vibronic models

This chapter introduces the methods used to calculate vibrationally resolved spectra. First, methods within the Born–Oppenheimer adiabatic approximation will be discussed in Sec. 5.1. Then in Sec. 5.2, I will proceed with describing a method based on a vibronic model Hamiltonian that is suitable when the adiabatic approximation breaks down.

5.1 Adiabatic approximation

Within the Born–Oppenheimer approximation, also known as the adiabatic approximation, a molecular wave function can be expressed as the product of an electronic wave function and a vibrational wave function, when only vibrational motion are considered for the nuclei. Following Ref. [45], I will let $\left|g\nu_g\right\rangle$ refer to the initial state and $\left|f\nu_f\right\rangle$ to the final state. Here ν_g and ν_f label the vibrational states of the electronic states g and f.

In Secs. 2.3–2.5, it was shown how spectral intensities are related to products and combinations of transition dipole moments. Starting with the electric dipole transition moment, this is then in the notation introduced above given by

$$\mu_\alpha^{g\nu_g f\nu_f} = \left\langle g\nu_g \left|\hat{\mu}_\alpha\right| f\nu_f \right\rangle . \tag{5.1}$$

Integrating over the electronic coordinates gives

$$\mu_\alpha^{g\nu_g f\nu_f} = \left\langle \nu_g \left| \mu_\alpha^{fg}(\mathbf{Q}) \right| \nu_f \right\rangle \tag{5.2}$$

where $\mathbf{Q}$ is the set of normal coordinates defined in Sec. 3.3.1. The electronic transition moment, $\mu_\alpha^{fg}(\mathbf{Q})$, may be expanded around the equilibrium geometry of the initial state

with respect to its normal coordinates as follows

$$\mu_\alpha^{fg}({}^g\mathbf{Q}) = \mu_\alpha^{fg}({}^g\mathbf{Q}_0) + \sum_a \frac{\partial \mu_\alpha^{fg}({}^g\mathbf{Q})}{\partial {}^gQ_a} {}^gQ_a + \cdots . \tag{5.3}$$

Inserting this expression into Eq. 5.2 gives

$$\mu_\alpha^{g\nu_g f\nu_f} = \mu_\alpha^{fg}({}^g\mathbf{Q}_0) \left\langle \nu_g \,|\, \nu_f \right\rangle + \sum_a \frac{\partial \mu_\alpha^{fg}({}^g\mathbf{Q})}{\partial {}^gQ_a} \left\langle \nu_g \,|{}^gQ_a| \nu_f \right\rangle + \cdots . \tag{5.4}$$

The magnetic dipole transition moment can be expressed in the same way as,

$$m_\alpha^{g\nu_g f\nu_f} = m_\alpha^{fg}(\mathbf{Q}_0) \left\langle \nu_g \,|\, \nu_f \right\rangle + \sum_a \frac{\partial m_\alpha^{fg}({}^g\mathbf{Q})}{\partial {}^gQ_a} \left\langle \nu_g \,|{}^gQ_a| \nu_f \right\rangle + \cdots . \tag{5.5}$$

The first term in Eqs. 5.4 and 5.5 consists of respectively the electric and magnetic transition moment at the equilibrium position of the ground state, multiplied with the overlap between the vibrational states, the so-called Franck–Condon factors. This term is referred to as the Franck–Condon (FC) contribution. The second term is called the Herzberg–Teller (HT) contribution and couples electronic states through the nuclear vibrations, giving rise to what is often called the "intensity-borrowing mechanism".[46] This mechanism may cause a non-zero intensity for transitions that are dipole-forbidden in the purely electronic picture (that is when $\mu_\alpha^{fg} = 0$ for $\alpha = x, y, z$), in addition to altering the intensity of other transitions.

The significance of the HT "intensity-borrowing mechanism" may be evaluated by writing the derivative of the electronic transition moment as [47]

$$\left(\frac{\partial \mu_\alpha^{fg}}{\partial {}^gQ_a}\right)_{\mathbf{Q}_0} = \left(\left\langle \frac{\partial \Theta_g}{\partial {}^gQ_a} \middle| \mu_\alpha^{fg} \middle| \Theta_f \right\rangle\right)_{\mathbf{Q}_0} + \left(\left\langle \Theta_g \middle| \mu_\alpha^{fg} \middle| \frac{\partial \Theta_f}{\partial {}^gQ_a} \right\rangle\right)_{\mathbf{Q}_0}, \tag{5.6}$$

where the derivatives of the electronic wave functions may be expanded as

$$\left(\frac{\partial \left|\Theta_n\right\rangle}{\partial {}^gQ_a}\right)_{{}^gQ_0} = -\sum_{m \neq n} \left(\frac{\left\langle \Theta_m \middle| \partial H^{\mathrm{el}} / \partial {}^gQ_a \middle| \Theta_n \right\rangle}{E_m - E_n}\right)_{{}^gQ_0} \left|\Theta_m\right\rangle . \tag{5.7}$$

It is seen from Eqs. 5.6 and 5.7 that when the final electronic state has a large energy separation with respect to other electronic states, the HT contribution will be small and the FC contribution will dominate.

The electronic states may also couple through the non-adiabatic operators in the molecular Hamiltonian (see Eq. 3.6). For electronic states that are close in energy, the

non-adiabatic operators may be quite significant, contributing to coupling terms that are substantially larger than the HT terms. In this case it is necessary to move beyond the adiabatic approximation. I will return to this situation in Sec. 5.2.

5.1.1 Analytical sum rules

To calculate a spectrum what is needed is then to insert Eqs. 5.4 and 5.5 into the final expressions in Sec. 2.3–2.5 and sum over all vibronic states in the region of interest. In practical calculations, it is not possible to include the overlaps of all vibrational states and the summation will therefore have to be truncated. The total intensity for a transition between two electronic states, can nevertheless be calculated analytically and this can be used to make sure that all non-negligible vibronic transitions have been included.

The total absorption intensity for the electronic transition $g \to f$ is from Eqs. 2.29 and 5.1 proportional to

$$\sum_{\nu_g,\nu_f} p_{\nu_g} \sum_{\alpha} \left| \mu_{\alpha}^{g\nu_g f\nu_f} \right|^2 = \sum_{\nu_g,\nu_f} p_{\nu_g} \sum_{\alpha} \left(\left\langle \nu_g \left| \mu_{\alpha}^{fg}({}^g\mathbf{Q}) \right| \nu_f \right\rangle \cdot \left\langle \nu_g \left| \mu_{\alpha}^{fg}({}^g\mathbf{Q}) \right| \nu_f \right\rangle \right), \quad (5.8)$$

where p_{ν_g} is the probability of the system initially being in the vibrational state ν_g. Inserting Eq. 5.4 truncated after the linear term, this may be shown to give [48]

$$\begin{aligned} \sum_{\nu_g,\nu_f} p_{\nu_g} \sum_{\alpha} \left| \mu_{\alpha}^{g\nu_g f\nu_f} \right|^2 = \sum_{\alpha} \Bigg[& \left(\mu_{\alpha}^{gf}({}^g\mathbf{Q}_0) \right)^2 \\ & + \sum_a \sum_{\nu_g} p_{\nu_g} \left(\frac{\partial \mu_{\alpha}^{fg}({}^g\mathbf{Q})}{\partial {}^gQ_a} \right)^2 \frac{1}{2\omega_a} (2\nu_{a,g} + 1) \Bigg], \end{aligned} \quad (5.9)$$

where ω_a is the frequency of normal mode a. The first term on the right-hand side above is the total Franck-Condon contribution, which is here just the product of the electric transition moment with itself. The second term is the total Herzberg-Teller contribution.

Similarly, we have from Eq. 2.38 that the total rotatory strength of ECD for the

electronic transition $g \to f$ is proportional to [45]

$$\sum_{\nu_g,\nu_f} p_{\nu_g} \sum_{\alpha} \mathrm{Im}\left(\mu_\alpha^{g\nu_g f\nu_f} \cdot m_\alpha^{g\nu_g f\nu_f}\right)$$

$$= \sum_{\nu_g,\nu_f} p_{\nu_g} \sum_{\alpha} \mathrm{Im}\left(\left\langle \nu_g \left| \mu_\alpha^{fg}({}^g\mathbf{Q}) \right| \nu_f \right\rangle \cdot \left\langle \nu_g \left| m_\alpha^{fg}({}^g\mathbf{Q}) \right| \nu_f \right\rangle\right) \tag{5.10}$$

$$= \sum_{\alpha} \mathrm{Im}\left[\mu_\alpha^{gf}({}^g\mathbf{Q}_0) m_\alpha^{gf}({}^g\mathbf{Q}_0)\right.$$

$$\left. + \sum_a \sum_{\nu_g} p_{\nu_g} \frac{\partial \mu_\alpha^{fg}({}^g\mathbf{Q})}{\partial {}^gQ_a} \frac{\partial m_\alpha^{fg}({}^g\mathbf{Q})}{\partial {}^gQ_a} \frac{1}{2\omega_a}(2\nu_{a,g}+1)\right]. \tag{5.11}$$

Again, the first term in 5.10 is the total FC contribution, while the latter is the HT contribution. It is noteworthy that there is no contribution from terms mixing the FC part of the electric transition moment and the HT part of the magnetic transition moment, or vice-versa. Another interesting feature is the possibility of "sign-inversion", where the HT contribution has the opposite sign of the FC contribution. This may give both positive and negative intensities for a single electronic state.

5.1.2 Adiabatic Franck–Condon

Within the adiabatic approximation, the main difference between the time-independent methods we will consider here lies, in addition to whether HT effects are included, in the description of the potential energy surfaces (PES) of the electronically excited states.

The (harmonic) adiabatic Franck–Condon model [49, 50, 51] is based on an harmonic analysis of the PES of each electronic state of interest around the equilibrium geometry of the respective state. It thus requires the optimization of the excited state geometry, as well as the calculation of the corresponding Hessian at this geometry. The expansion may also in principle be expanded to include anharmonicities, but this has not been done in the applications of AFC in the present work.

Restricting the description of the excited state PES to the harmonic approximation, the sets of normal coordinates for the initial state g and finale state f are related by the linear transformation [52]

$$ {}^g\mathbf{Q} = \mathbf{J}^f\mathbf{Q} + \mathbf{K}, \tag{5.12}$$

where $\mathbf{J}$ is the Duschinsky matrix that describes the rotation between the ground- and excited state normal modes and $\mathbf{K}$ is a vector describing displacement from the ground

state equilibrium geometry. The Duschinsky matrix and the displacements vector are given by

$$\mathbf{J} = \mathbf{L}^{g,-1}\mathbf{L}^{f} \tag{5.13}$$

$$\mathbf{K} = \mathbf{L}^{g,-1}({}^{f}\mathbf{Q}_0 - {}^{g}\mathbf{Q}_0), \tag{5.14}$$

where $\mathbf{L}^g$ and $\mathbf{L}^f$ are the normal coordinate matrix of the initial and final state, respectively, and ${}^f\mathbf{Q}_0$ and ${}^g\mathbf{Q}_0$ the equilibrium normal coordinates of the same states.

It should here be noted that though the three translational coordinates can be eliminated exactly from Eq. 5.12, this is in general not the case for the rotational coordinates. The mixing of the rotational and vibrational coordinates can, however, be minimized by through a suitable rotation of one of the two equilibrium structures. This can be achieved by minimizing the root-mean-square distance (RMSD) of the molecular nuclei in the two equilibrium positions, which in one approach can be done using quaternions.[53]

Since in general the Duschinsky matrix $\mathbf{J}$ is not diagonal, the multidimensional FC overlaps cannot be separated in a product of one-dimensional integrals. The overlaps can, however, be calculated recursively using either the generating functions approach of Sharp and Rosenstock [54] or the coherent state approach of Doktorov *et al.* [55] Here, the former approach has been used. The form of the one-dimensional integrals will be discussed in the next section.

An aspect that may make calculations challenging, is the huge number of vibrational states that may contribute to the spectra. In most cases, however, the contributions from the majority of the excited states will be neglible. This means that it is beneficial, and indeed, crucial when going to larger systems, to adopt a strategy for preselecting the important integrals.

In the calculation of vibrationally resolved spectra within the adiabatic approximation in the present work, the program FCclasses [56] has been employed to calculate the vibronic intensities. This program performs a prescreening of which FC integrals to include in the calculation by collecting transitions to the manifold of vibrational states $\left|\nu_f\right\rangle$ into classes C_n, where n is the number of vibrational modes with a non-zero quantum number.[48, 57, 58, 59] Selection schemes are then employed to determine the maximum number of quanta to include in each class. Convergence can finally be tested by comparison with the result of the analytical sum rules in Sec. 5.1.1. It is noted that a more rigorous method for prescreening FC integrals has been proposed by Jankowiak *et al.* [60]

5.1.3 Vertical gradient model

The computational demands of the AFC model, which includes the optimization of excited states, makes it unfeasible for larger systems. A more simplistic model is provided by the vertical gradient (VG) model,[61] sometimes referred to as the linear coupling model (LCM). In this approximation, it is assumed that the ground and excited states have the same harmonic PES apart from a small displacement of the equilibrium coordinates. That is, the excited state will have the same set of normal modes as the ground state, with the only difference that each excited state normal mode a will be displaced by a distance ΔQ_a. This displacement can be calculated from the excited state gradient,

$$\Delta Q_a = -\frac{1}{\omega_a^2}\frac{\partial E_f(\mathbf{Q})}{\partial Q_a}. \tag{5.15}$$

In contrast to the AFC model, the FC factors will in the VG model be given as products of displaced one-dimensional harmonic oscillator overlap integrals

$$\langle \nu_g \,|\, \nu_f \rangle = \prod_a \langle \nu_{a,g} \,|\, \nu_{a,f} \rangle . \tag{5.16}$$

Assuming that $\nu_{a,g} \leq \nu_{a,f}$, these one-dimensional overlap integrals are given by

$$\langle \nu_{a,g} \,|\, \nu_{a,f} \rangle = (-1)^{\nu_{a,f}-\nu_{a,g}} e^{\frac{x_a^2}{2}} x_a^{(\nu_{a,f}-\nu_{a,g})} \sqrt{\frac{\nu_{a,g}!}{\nu_{a,f}!}} L_{\nu_{a,g}}^{\nu_{a,f}-\nu_{a,g}}(x_a), \tag{5.17}$$

where x_a is a dimensionless factor relating the displacements and the frequencies, and $L_{\nu_{a,g}}^{\nu_{a,f}-\nu_{a,g}}(x_a)$ is the associated Laguerre polynomial.

$$L^{\nu_{a,f}-\nu_{a,g}}(x_a) = \sum_{r=0}^{\nu_{a,g}} \frac{\nu_{a,f}!(-x_a^2)^r}{(\nu_{a,g}-r)!(\nu_{a,f}-\nu_{a,g}+r)!r!}. \tag{5.18}$$

The integrals involved in the Herzberg–Teller contribution will also be given as products of one-dimensional integrals,

$$\langle \nu_g \,|Q_a|\, \nu_f \rangle = \langle \nu_{a,g} \,|Q_a|\, \nu_{a,f} \rangle \prod_{b\neq a} \langle \nu_{b,g} \,|\, \nu_{b,f} \rangle , \tag{5.19}$$

where the one-dimensional integral over the normal coordinate Q_a is related to the FC factors by

$$\langle \nu_{a,g} \,|Q_a|\, \nu_{a,f} \rangle = \frac{1}{2\omega_a}\left(\sqrt{\nu_{a,g}+1}\, \langle \nu_{a,g}+1 \,|\, \nu_{a,f} \rangle + \sqrt{\nu_{a,g}}\, \langle \nu_{a,g}-1 \,|\, \nu_{a,f} \rangle \right). \tag{5.20}$$

The assumption that the curvature of the excited states is the same as that of the ground state is of course a rather crude approximation to the excited state PES. Nevertheless, the benefits of the VG model include quite easily obtainable excited state surfaces, as well as a simple form for the overlap integrals contributing to the intensities. This makes the model applicable to much larger systems than the AFC model which provides a more accurate description of the excited state surfaces. For reasons that will be clear from the discussion in Sec. 5.1.4, the VG model will typically be able to capture the most important features of vibrationally resolved spectra.

5.1.4 Vertical Franck–Condon

The approach used in the VG model may be extended by performing a harmonic analysis of the excited state surfaces around the equilibrium geometry of the ground state. This gives the vertical Franck–Condon (VFC) [62] model, which avoids the cumbersome optimization of the excited state geometries needed in the AFC model, while providing a better description of the excited state surfaces than the VG model since it includes Duschinsky rotation. Although no applications of the VFC model have been made in this work, it might be useful to mention some aspects of the motivation for the model, since it provides a connection between the models within the adiabatic approximation and the model discussed below which goes beyond this approximation.

The motivation for the VFC model comes from the time-dependent picture of spectroscopy,[63, 64] where the excited wave function is understood as a localized wave packet evolving on the excited-state surfaces before finally decaying back to ground state. The spectrum can be obtained from a Fourier transform of the time-correlation function $C(t)$ for the process,

$$C(t) = \langle \Psi(0) \,|\, \Psi(t) \rangle \,, \tag{5.21}$$

where $\Psi(t)$ is the evolving wave packet. It is only necessary to know the time-correlation time function for a short time (50–100 fs) to simulate the absorption, though the resolution of the spectrum will be better with increasing simulation time. In particular we have that both the maximum and the width of the absorption envelope, the "band" corresponding to a transition to an electronic state, come from short features in time.

In the short-time picture, the wave packet will probe only the region of the excited state close to the ground state equilibrium geometry, the so-called Condon region. To describe the broad features of the spectrum accurately, what is needed is therefore a good

description of the excited-state PES in the Condon region. This is exactly what the VFC model aspires to provide, in contrast to the AFC model based on an expansion around the excited state equilibrium geometry. It is therefore expected that the broad features of the spectrum will be better described by VFC, while AFC will give better results for low-lying transitions in particular. In the limit where the harmonic approximation holds exactly, the two approaches will be equivalent. The VG model, like the VFC model based on a vertical approach, will typically also give an adequate description of the broad features of the spectrum, though of course in a less accurate manner than the VFC model.

5.2 Vibronic model Hamiltonian

As mentioned above, the adiabatic approximation tends to break down when electronic states are close in energy. It is then necessary to include the coupling of the electronic states in the Hamiltonian. Since the nonadiabatic coupling elements are complicated to calculate and may even be divergent, it is beneficial to switch to a basis that minimizes these. In the following, I will first discuss the diabatic basis chosen for the vibronic model before proceeding with describing how spectra are obtained in this model.

5.2.1 The diabatic basis

Following the review by Köppel *et al.*,[11] the molecular Schrödinger equation in Eq. 3.6 may be written in matrix form. If the electronic states are chosen to be in the adiabatic representation, as has been done so far, the corresponding matrix Hamiltonian is given as

$$\mathcal{H} = \hat{T}_{\text{nuc}}\mathbf{1} + \mathbf{V}(Q) + \lambda(Q), \tag{5.22}$$

where $\mathbf{V}$ is a diagonal matrix of electronic energies

$$V_{mn}(Q) = \delta_{mn}E_n(Q), \tag{5.23}$$

and $\lambda(Q)$ are the non-adiabatic coupling matrix with elements given by Eq. 3.7.

When the electronic states are well separated, the adiabatic approximation is valid since the non-adiabatic coupling matrix elements will be negligible. On the other hand, when the separation between the electronic states is small, i.e for near-degeneracies,

conical intersections and avoided crossings, the coupling matrix elements can become very large and even divergent. In such cases, this coupling may not be neglected.

The adiabatic states rapidly change character in the vicinity of conical intersections and avoided crossings. This gives rise to the complicated behavior of the non-adiabatic coupling matrix elements in such regions. In addition, these coupling elements are quite cumbersome to calculate. One solution to this problem is to switch to a basis of states that are smooth functions of the nuclear coordinates and that are allowed to cross at the avoided crossings of the adiabatic states. Such states are referred to as diabatic electronic states.

In the diabatic basis, the matrix Hamiltonian can be written as

$$\mathcal{H} = \hat{T}_{\text{nuc}}\mathbf{1} + \mathbf{W}(Q), \tag{5.24}$$

where

$$W_{nm} = \left\langle \phi_n(Q) \left| \hat{H}_{\text{el}} \right| \phi_m(Q) \right\rangle. \tag{5.25}$$

Here, $|\phi_n(Q)\rangle$ refers to diabatic states, and it is assumed that these states are obtained in such a way that the coupling elements λ can be neglected in this basis. The electronic states are now instead coupled through $\mathbf{W}(Q)$, which in general is not diagonal.

The elements of the potential energy matrix $\mathbf{W}$ are, in contrast to what is the case for the adiabatic states, slowly varying functions of Q, and one can therefore expand $(\mathbf{W} - E_0\mathbf{1})$ about a reference geometry Q_0 as follows

$$\mathcal{H}_{nn} = \hat{T}_{\text{nuc}} + E_0(Q) + [E_n(Q_0) - E_0(Q_0)] + \sum_s \kappa_s^{(n)} Q_s + \cdots \tag{5.26}$$

$$\mathcal{H}_{nm} = \sum_s \lambda_s^{(n,m)} Q_s + \cdots. \tag{5.27}$$

In the above expansion, $\kappa_s^{(n)}$ and $\lambda_s^{(n,m)}$ are called intrastate and interstate coupling constants respectively, and Q_s refer to a displacements along normal modes s.

In practice, the diabatic matrix Hamiltonian is constructed for a subset of the electronic states, and the vibronic coupling problem will only be solved for the states within the subset.

5.2.2 Diabatization scheme

Diabatic states are in general not uniquely defined. The main approach employed in the present work is based on the overlap between excited-state wave functions calculated

at the reference geometry and at displaced nuclear geometries.[65] At each displaced geometry, Δ, an overlap matrix S is calculated

$$S_{ab} = \langle \Phi_a(\Delta) \,|\, \Phi_b(0) \rangle \,, \tag{5.28}$$

where $\Phi_a(\Delta)$ is an adiabatic excited state at the displaced geometry and $\Phi_b(0)$ an adiabatic excited state at the reference geometry. The exact form of the this overlap when the excited states are obtained from response theory, as is the case for TDDFT, is given in Ref. [66]. It is noted that since the molecular orbitals themselves are geometry dependent, the overlap must be calculated in the atomic orbital basis.

Diabatic states ϕ_c are then defined by the unitary transformation

$$|\phi_c(\Delta)\rangle = \sum_a U_{ca} \, |\Phi_c(\Delta)\rangle \tag{5.29}$$

that minimizes the off-diagonal elements of the overlap matrix. At the reference geometry the diabatic and adiabatic states are defined to be equal.

The adiabatic potential energy matrix and transition moments can then be transformed to the diabatic basis

$$W_{cb}(\Delta) = \sum_a U_{ca} E_a(\Delta) U_{ab} \tag{5.30}$$

$$\tau_n(\Delta) = \sum_a U_{ca} \tilde{\tau}_a(\Delta), \tag{5.31}$$

where I have introduced $\tilde{\tau}$ and τ as a column vectors of general electronic transition moments $\tilde{\tau}_n$ and τ_n, in respectively the adiabatic and the diabatic basis. Using the diabatic transition moments as an example, these are defined for an operator $\hat{T}$ by

$$\tau_n = \left\langle \phi_0 \left| \hat{T} \right| \phi_n \right\rangle . \tag{5.32}$$

Numerical differentiation is then used to obtain the vibronic coupling constants. Small nuclear displacements $\Delta = dQ_i$ and $\Delta = 2dQ_i$ along normal coordinates Q_i are used to extract up to quartic diagonal coupling constants and displacements $\Delta = dQ_i dQ_j$ to extract off-diagonal quadratic coupling constants in Eqs. 5.26 and 5.27. If we disregard the interstate coupling, the off-diagonal coupling constants account for Duschinsky rotation, while the diagonal higher-order couplings describe anharmonicities.

5.2.3 The vibronic absorption and CD spectra

If the molecular ground state is well separated from the electronically excited states, the one-photon absorption probability can from the golden rule (see Eq. 2.25) be given as [11, 67]

$$P(\omega) = \frac{\pi}{2}\sum_{\nu} \left|\left\langle \Psi_0 \left| \hat{T} \right| \Psi_\lambda \right\rangle\right|^2 \delta(\omega - \omega_\nu) \tag{5.33}$$

where Ψ_0 and Ψ_λ are the exact states of the system, the summation running over all excited states. The interactions of the electrons with the electromagnetic field are here described by the operator $\hat{T}$. Eq. 5.33 may be rewritten in a time-dependent form that does not explicitly include the final states and energies as follows

$$P(\omega) = \frac{1}{4}\int_{-\infty}^{\infty} e^{i\omega t} \left\langle \Psi_0 \left| \hat{T} e^{-iHt} \hat{T}^\dagger \right| \Psi_0 \right\rangle dt, \tag{5.34}$$

where the auto-correlation function in Eq. 5.21 is given in terms of the time-independent ground-state wave function so that

$$C(t) = \left\langle \Psi_0 \left| \hat{T} e^{-iHt} \hat{T}^\dagger \right| \Psi_0 \right\rangle. \tag{5.35}$$

The time-dependent approach will not be used directly here. Instead the auto-correlation function will be described by a model Hamiltonian that can be diagonalized to obtain the spectrum. This is achieved by representing both the real Hamiltonian and the ground state in the diabatic basis,

$$H = \sum_{n,m} |\phi_n\rangle \mathcal{H}_{nm} \langle\phi_m| \tag{5.36}$$

$$\Psi_0 = \chi_0(\mathbf{Q})\phi_0(\mathbf{r},\mathbf{Q}), \tag{5.37}$$

where it is assumed that the adiabatic approximation holds for the electronic ground state. $|\chi_0\rangle = |\chi_{00}\rangle$ is the nuclear ground state.

In terms of this model Hamiltonian, the excitation spectrum is now given by

$$P(\omega) = \frac{1}{4}\int_{-\infty}^{\infty} e^{i\omega t} \left\langle \chi_0 \left| \tau^\dagger e^{-i\mathcal{H}t} \tau \right| \chi_0 \right\rangle dt, \tag{5.38}$$

which when integrated over time gives

$$P(\omega) = \frac{\pi}{2} \left\langle \chi_0 \left| \tau^\dagger \delta(\omega - \mathcal{H}) \tau \right| \chi_0 \right\rangle. \tag{5.39}$$

The matrix Hamiltonian $\mathcal{H}$ will be represented in the basis of the vibrational states introduced in Sec. 3.3 which are eigenstates for the nuclear Hamiltonian in the electronic ground state. Simplifying Eq. 3.18, the compact notation

$$|\mathbf{n}\rangle = |n_1 n_2 \cdots n_{3N-6}\rangle \tag{5.40}$$

will here be used to denote a vibrational state for the electronic state ϕ_n, where n_s are the vibrational wave number or quanta in mode s. If M electronic states are included in the vibronic model, a supermatrix with $M \times M$ matrices $\mathcal{H}_{\mathbf{nm}}$ as elements is obtained

$$\mathcal{H}_{\mathbf{nm}} = \langle \mathbf{n} | \mathcal{H} | \mathbf{m} \rangle . \tag{5.41}$$

The absorption spectrum can from Eq. 5.39 now be obtained by diagonalizing the matrix Hamiltonian $\mathcal{H}$ in this basis. This gives the vibronic eigenstates,

$$|\psi_\lambda\rangle = \sum_{\mathbf{n},a} |\mathbf{n}, a\rangle \, c^\lambda_{\mathbf{n},a}, \tag{5.42}$$

where a labels the diabatic electronic states. The corresponding eigenvalues gives the vibronic excitation energies, ω_λ. Inserting this expression for the final vibronic states into Eq. 2.33 and 2.38 gives respectively the expressions for the oscillator strength of regular absorption spectroscopy and the rotational strength of ECD,[68]

$$f_{0\lambda} = \frac{2\omega_\lambda}{3} \sum_\alpha \sum_a \left| c^\lambda_{\mathbf{0},a} \mu^{0a}_\alpha \right|^2 \tag{5.43}$$

$$R_{0\lambda} = \sum_\alpha \sum_a \left| c^\lambda_{\mathbf{0},a} \right|^2 \mathrm{Im} \left(\mu^{0a}_\alpha \cdot m^{0a}_\alpha \right) . \tag{5.44}$$

Since the diabatic states have been constructed to vary slowly with the geometry, it has here been assumed that the transition moments are geometry independent in the diabatic basis. The simulation of the MCD spectrum based on the vibronic model the will not be discussed here, but it should be mentioned that a time-dependent approach to vibronic MCD recently was presented by Lee *et al.*[69]

Note that the dimension of $\mathcal{H}_{\mathbf{nm}}$ depends on the number of vibrational modes of the system studied and on how many quanta n_s we allow in each normal mode, which means that this quickly becomes a very large matrix to diagonalize.

In this work, the Lanzcos algorithm have been used to diagonalize the matrix Hamiltonian [65, 70] using the VIBRON program.[71] The Lanzcos algorithm is an iterative method that is especially suitable for large, sparse matrices like we have here. The computationally effort needed for the diagonalization might still be considerable and a judicious choice of the maximum quanta allowed in each normal mode is needed.

Chapter 6

Summary of papers

This chapter presents a summary of the papers included in this dissertation and the main results obtained. In Secs. 6.1–6.3, results obtained at the electronic level is presented. Here, the focus will be on MCD in Papers I–III, while in Paper IV results for both absorption, CD, and MCD spectra are presented in a more applied study. The attention then turns to vibrationally resolved spectra in Secs. 6.4–6.5. Paper V presents calculations of CD for a molecule with isotopically engendered chirality. In Paper VI, aspects of the construction of an accurate vibronic model Hamiltonian are discussed.

6.1 Solvent and correlation effects on the MCD $\mathcal{B}$ term

In Paper I, the first theoretical investigation of solvent effects on the MCD $\mathcal{B}$ term at the DFT level is presented. The $\mathcal{B}$ term has here been calculated from the single residue of a quadratic response function as described in Sec. 4.4. Results for four different benzoquinones obtained both at the Hartree–Fock level and the DFT level using several functionals are discussed. It is seen that inclusion of correlation effects are crucial to get qualitative agreement with experiment.

As an example, the results for the first dipole-allowed electronic transition in *para*-benzoquinone are collected in Table 6.1.1. It is seen that at the Hartree–Fock level, which does not include electron correlation, even the sign of the $\mathcal{B}$ term is not correct. The sign is, however, predicted correctly by all the DFT functionals shown here. Nevertheless, the intensity of the transition is grossly overestimated by most of the functionals. For all the molecules included in the study, the $\mathcal{B}$ term shows a strong sensitivity to the amount

	Wavelength	$\mathcal{B}$ term
Hartree–Fock	203 (211)	6.78 (8.73)
B3LYP	251 (257)	-3.75 (-4.41)
CAM-B3LYP	234 (240)	-2.21 (-2.20)
BHLYP	227 (234)	-1.31 (-0.99)
BLYP	279 (278)	-3.88 (-6.12)
KT1	269 (275)	-2.66 (-4.68)
KT2	269 (275)	-4.76 (-4.88)
KT3	269 (275)	-4.74 (-5.27)
Experiment (Ref. [72])	(241)	(-0.68)

Table 6.1.1: Excitation wavelength in nm and MCD $\mathcal{B}$ term in a.u. in gas phase and, in paranthesis, *n*-hexane for the X $^1\mathrm{A}_g \rightarrow 1\ ^1\mathrm{B}_u$ transition in *para*-benzoquinone. Basis set aug-cc-pVTZ.

of exact exchange included in the functional. This can be seen from a comparison of the results for B3LYP, CAM-B3LYP, and BHLYP in our example. BHLYP, which includes the largest amount of exact exchange, predicts the smallest negative intensity for the $\mathcal{B}$, while B3LYP, which includes the lowest amount of exact exchange, predicts the largest negative intensity of these three functionals.

Another interesting observation is that while in most cases dielectric continuum effects increase the value of the $\mathcal{B}$ term, in some cases a decrease in this value upon solvation is predicted. In Table 6.1.1, such a decrease is seen for CAM-B3LYP and BHLYP. This effect is caused by an interplay of correlation and solvation effects on the individual contributions to the $\mathcal{B}$ term.

6.2 MCD $\mathcal{A}$ and $\mathcal{B}$ terms from damped response theory

Traditionally, the temperature-independent part of MCD spectra have been rationalized in terms of the Faraday $\mathcal{A}$ and $\mathcal{B}$ terms, which I above have called the MCD $\mathcal{A}$ and $\mathcal{B}$ terms. The $\mathcal{A}$ term is then only observed for systems with degenerate states, while the $\mathcal{B}$ term contributes to the MCD spectra for all molecules. In Papers II and III, calculations based on damped response theory are presented as an alternative and unified approach for the time-independent contributions to the spectrum at the electronic level.

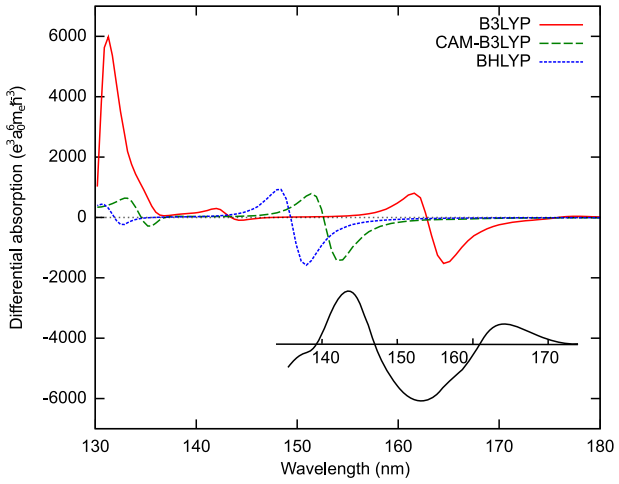

Figure 6.1: Calculated MCD spectra of cyclopropane. The excited-state lifetime broadening is set to 1000 cm^{-1}, and the frequencies have been calculated with a separation of 0.001 Hartree. The *inset* shows the experimental spectrum from Ref. [73].

Paper II demonstrates that the appropriate quadratic complex response function (see Eq. 4.44) can account for both the $\mathcal{A}$ and $\mathcal{B}$ terms of MCD. The example systems used are *para*-benzoquinone and tetrachloro-*para*-benzoquinone, which belonging to the D_{2h} point group will only have contributions from the $\mathcal{B}$ term, and cyclopropane, where contributions from the $\mathcal{A}$ term will be present, and likely dominate the spectrum, since it belongs to the D_{3h} point group.

For the benzoquinones, it is demonstrated that the simulation based on damped response theory reproduces the results of the calculations in Paper I when suitable Lorentzian lineshape functions are added to the calculated $\mathcal{B}$ term intensities of the latter. As for cyclopropane it is seen that the calculated spectra have features that can be attributed to $\mathcal{A}$ term contributions. In Fig. 6.1, this is most clearly seen for the $2E'$ state, whose vertical excitation wavelength is predicted to be 164.0 nm by B3LYP, 153.3 nm by CAM-B3LYP, and 150 nm by BHLYP. The experimental spectrum also has a distinct band that may be attributed to the $1E'$ state. Calculations based on the mentioned DFT functionals predict low intensity for this state, and thus fail to reproduce this part of the spectrum.

This work is followed up in Paper III, where a proposal is made for the abandonment of the historical separation of the temperature-independent part of the MCD spectrum into an $\mathcal{A}$ and a $\mathcal{B}$ term. This separation stands in contrast to most other birefringencies

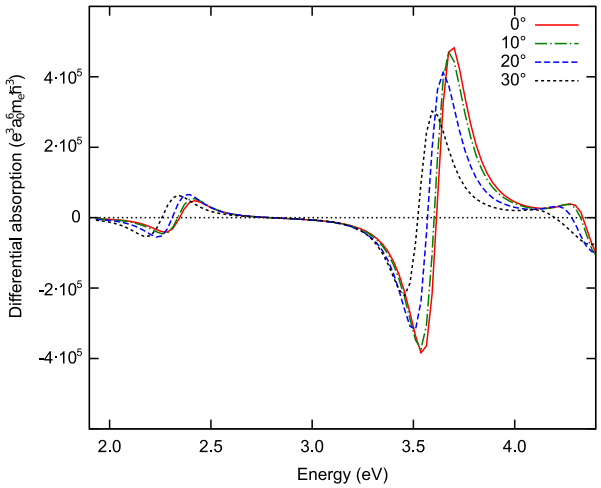

Figure 6.2: Calculated MCD spectra of Zn-porphyrin bent about the meso-carbon–metal–meso-carbon axis obtained using the aug-cc-pVDZ basis set and the CAM-B3LYP functional.

where the temperate-independent part are described by a single term.[74] It is argued that the separation in $\mathcal{A}$ and $\mathcal{B}$ terms is artificial and may lead to incorrect analysis of the nature of excited states in highly symmetric systems.

The artificialness of this separation may be illustrated by looking at small geometrical distortions of a highly symmetric system, as shown in an exaggerated manner for Zn-porphyrin in Fig. 6.2. In the fully symmetric D_{4h} system, the dominant contributions will typically arise from the $\mathcal{A}$ terms of the degenerate states. However, when the symmetry is reduced, the degeneracies will be lifted and the spectrum may now only contain $\mathcal{B}$ terms. The MCD spectrum will still show a derivative band shape, which in this case will be described as due to overlapping $\mathcal{B}$ terms, often referred to as a pseudo-$\mathcal{A}$ term. From Fig. 6.2, it observed that even for the rather severe geometry distortion of 30°, the features of the original spectrum is retained.

6.3 Absorption, CD, and MCD of cobalamins

Studies of the excited electronic states of cobalamins have been an active field of research lately. Still there are open questions related to the assignment of the bands in spectra of these systems. So far the theoretical studies have been performed at the DFT level and

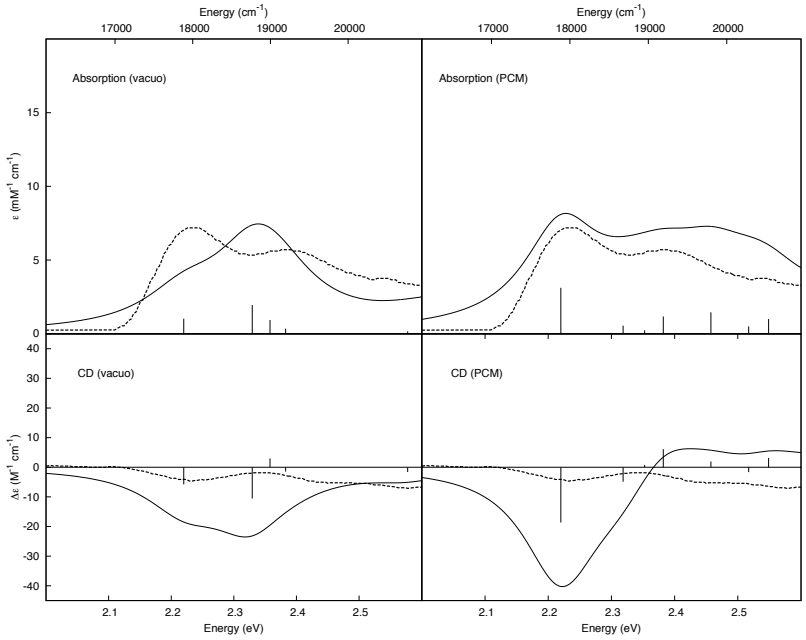

Figure 6.3: Comparison of low-energy regions of CNCbl absorption and CD spectra computed with BP86/aug-cc-pVDZ. Experimental data were taken from Ref. [75].

only considering the absorption spectra. CD and MCD spectra can provide information complementary to that given by regular absorption spectroscopy, and in the study of cyanocobalamin (CNCbl), known as Vitamin B_{12}, and methylcobalamin (MeCbl) in Paper IV, calculations of the CD and MCD spectra, in addition to absorption spectra, have been performed.

Usually the absorption spectra of cobalamins are discussed in terms of four main bands, labelled α/β, D/E, γ, and δ, respectively. In Paper IV, results for the three first of these bands are analyzed, with particular attention given to the low-energy α/β band. At the DFT level, calculations were performed on truncated models of the two systems studied, and results for gas phase and solution were compared. A simple scaling procedure was applied to the calculated excitation energies to ease the comparison with experiment.

Of the two functionals included in the study, BP86 and CAM-B3LYP, the best agreement with experiment overall was found for BP86. Focusing on the α/β band, the band shape was found to be strongly affected by solvent effects for CNCbl as shown in Fig. 6.3, but less so for MeCbl. This difference may be due to the more ionic character of

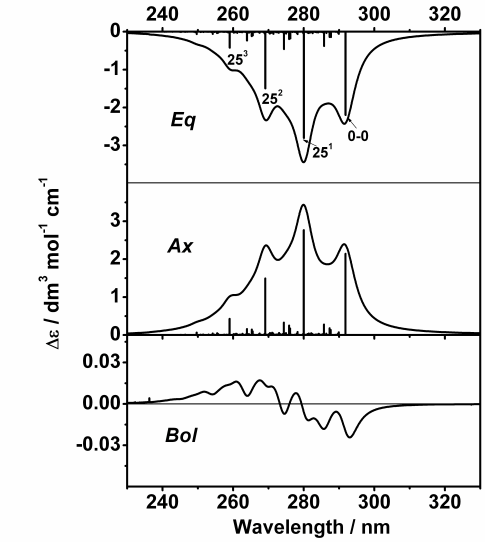

Figure 6.4: Calculated CD spectra of 2RDCP based on AFC in the region of the first excited state. The equatorial (Eq) conformer is shown in the upper panel, the axial (Ax) conformer in middle panel, and the Boltzmann averaged spectrum, assuming an equal weight of the two conformers, in the middle panel.

CNCbl in polar solvents. For CnCbl, the α/β band has traditionally been interpreted as a vibrational progression associated with a single electronic state, but the BP86 calculations including solvent effects presented here, suggest that the band is better interpreted as consisting of multiple electronic transitions.

6.4 Isotopically engendered chirality

The final two papers presented in this dissertation address the calculation of vibrationally resolved spectra. The first of these is a study of the CD spectrum for an isotopically substituted molecule. In Paper V, calculations both at the adiabatic level, using the vertical gradient model and AFC, and beyond, using the vibronic model Hamiltonian, are presented for 2(*R*)-deuteriocyclopentanone (2RDCP). In equilibrium, 2RDCP has two distinct, but near isoenergetic, half-chair conformations, which complicates the calculations. Without the substituted deuterium, the two conformations will actually be

enantiomers of each other and the CD signals would cancel each other. For 2RDCP, this cancellation is no longer complete, even when it is assumed that the two conformers will have the same Boltzmann population. An interesting aspect is that the comparison between the experimental and simulated CD spectra may help determine the Boltzmann weight of each conformer. This weight is hard to predict from energy calculations alone due to the small energy difference between the conformers.

In Fig. 6.4, simulated spectra based on the AFC model assuming an equal distribution of the two conformers, are shown for the first excited state. This illustrates how the CD signals from the two conformers nearly cancel each other, emphasizing the need for an accurate description of the potential energy surfaces. This state has a quite large energy separation from higher-lying states, so for this band nonadiabatic effects are less important.

The low-wavelength region of the spectrum has contributions from four electronic states, where in particular two of the states are very close in energy. For this region, the inclusion of vibronic coupling effects is expected to be essential, and this is confirmed by a comparison of the results from the VG model and the vibronic model.

6.5 Systematic construction of vibronic coupling Hamiltonians

Vibronic coupling phenomena is frequently observed in molecular spectroscopy due to the breakdown of the Born–Oppenheimer approximation. In Paper VI, the systematic construction of vibronic coupling Hamiltonians is discussed using the 1^1B_{3u} and 1^1B_{2u} states of pyrazine as an example. For an accurate treatment of the excited-state potential-energy surfaces in this system, inclusion of nondynamical correlation is necessary. In contrast to the papers discussed above where DFT was employed, calculations have therefore here been performed using wave-function based correlated methods. The ground-state force field was obtained at the MP2, CASPT2 and CCSD levels, while NEVPT2, CASPT2, MRCI and similarity transformed EOM-CCSD was used to analyse the excited-state PES.

The focus in this study is on aspects that are important for the derivation of accurate approximations of the potential energy surfaces, and to a lesser degree on the actual simulation of the vibronic spectra. Indeed, in the version of the manuscript included

in this dissertation, simulated spectra have not been included. Spectra are, however, planned to be included in the final version of the manuscript.

Vibronic coupling parameters are obtained by making displacements along normal mode-like coordinates. In a strict sense, a normal coordinate is only defined for infinitesimal displacement from a stationary point so any finite displacement is necessarily approximate. Usually this is done by evaluating linearized shifts away from the reference geometry along Cartesian normal coordinate vectors. In the present study, this approach has been compared with using curvilinear coordinates to represent displacements along the normal coordinate.

The need for consistency in the methodology used for computing the excited-state potential energy surfaces is also discussed. Ideally, the same method should be used both for obtaining the ground-state reference geometry and force field and the excitation energies. Due to limitations in various electronic structure models, this will not always be realizable. Results presented in this study indicate that in some cases, the effects of both the approximation used for normal-coordinate displacements and the level of consistency between different electronic structure models employed may be larger than expected.

Bibliography

[1] Barron, L. D. *Molecular Light Scattering and Optical Activity;* Cambridge University Press, 2nd ed., 2004.

[2] Michl, J.; Thulstrup, E. W. *Spectroscopy with Polarized Light: Solute Alignment by Photoselection, in Liquid Crystals, Polymers, and Membranes;* Wiley, 1995.

[3] Rizzo, A.; Coriani, S.; Ruud, K. In *Computational Strategies for Spectroscopy: from Small Molecules to Nano Systems*; Barone, V., Ed.; Wiley, 2011.

[4] Atkins, P. W.; Friedman, R. S. *Molecular Quantum Mechanics;* Oxford University Press, 3rd ed., 1997.

[5] Craig, D. P.; Thirunamachandran, T. *Molecular Quantum Electrodynamics;* Dover Publications, Inc., 1998.

[6] Thulstrup, E. W.; Michl, J. *Elementary polarization spectroscopy;* Wiley, 1989.

[7] Serber, R. *Phys. Rev.* **1932**, *147*, 489.

[8] Stephens, P. J. *Chem. Phys. Lett.* **1968**, *2*, 241.

[9] Stephens, P. J. *J. Chem. Phys.* **1970**, *52*, 3489.

[10] Szabo, A.; Ostlund, N. S. *Modern Quantum Chemistry: Introduction to Advanced Electronic Structure Theory;* Dover Publications, Inc., 1996.

[11] Köppel, H.; Domcke, W.; Cederbaum, L. S. *Adv. in Chem. Phys.* **1984**, *57*, 59.

[12] Wilson, E. B.; Decius, J. C.; Cross, P. C. *Molecular Vibrations: The Theory of Infrared and Raman Vibrational Spectra;* Dover, 1 ed., 1980.

[13] Helgaker, T.; Jørgensen, P.; Olsen, J. *Molecular Electronic-Structure Theory;* Wiley, 2000.

[14] Andersson, K.; Malmqvist, P.-Å.; Roos, B. O.; Sadley, A. J.; Wolinski, K. *J. Chem. Phys.* **1990**, *94*, 5483.

[15] Andersson, K.; Malmqvist, P.-Å.; Roos, B. O. *J. Chem. Phys.* **1992**, *96*, 1218.

[16] Angeli, C.; Cimiraglia, R.; Evangelisti, S.; Leininger, T.; Malrieu, J.-P. *J. Chem. Phys.* **2001**, *114*, 10252.

[17] Hohenberg, P.; Kohn, W. *Phys. Rev.* **1964**, *136*, B864.

[18] Saue, T.; Helgaker, T. *J. Comput. Chem* **2002**, *23*, 814.

[19] Becke, A. D. *J. Chem. Phys.* **1993**, *98*, 1372.

[20] Perdew, J. P.; Ernzerhof, M.; Burke, K. *J. Chem. Phys.* **1996**, *105*, 9982.

[21] Miertus, S.; Scrocco, E.; Tomasi, J. *Chemical Physics* **1981**, *55*(1), 117 – 129.

[22] Cammi, R.; Tomasi, J. *J. Comput. Chem* **1995**, *16*, 1449.

[23] Cancès, E.; Mennucci, B.; Tomasi, J. *J Chem Phys* **1997**, *107*, 3032.

[24] Mennucci, B.; Cancès, E.; Tomasi, J. *J Phys Chem B* **1997**, *101*, 10506.

[25] Cancès, E.; Mennucci, B. *J. Math. Chem.* **1998**, *23*, 309.

[26] Cammi, R.; Frediani, L.; Mennucci, B.; Tomasi, J.; Ruud, K.; Mikkelsen, K. *J. Chem. Phys.* **2002**, *117*, 13.

[27] Frediani, L.; Ågren, H.; Ferrighi, L.; Ruud, K. *J. Chem. Phys* **2005**, *123*, 144117.

[28] Olsen, J.; Jørgensen, P. *J. Chem. Phys.* **1985**, *82*, 3235.

[29] Norman, P.; Bishop, D. M.; Jensen, H. J. A.; Oddershede, J. *J. Chem. Phys.* **2005**, *123*, 194103.

[30] Sasagane, K.; Aiga, F.; Itoh, R. *J. Chem. Phys.* **1993**, *99*, 3738.

[31] Christiansen, O.; Jørgensen, P.; Hättig, C. *Int. J. Quantum Chem.* **1998**, *68*, 1.

[32] Ehrenfest, P. *Z. Phys.* **1927**, *45*, 455.

[33] Sałek, P.; Vathras, O.; Helgaker, T.; Ågren, H. *J. Chem. Phys.* **2002**, *117*, 9630.

[34] London, F. *J. Phys. Radium.* **1937**, *8*, 397.

[35] Bak, K. L.; Hansen, A. E.; Ruud, K.; Helgaker, T.; Olsen, J.; Jørgensen, P. *Theor. Chim. Acta* **1995**, *90*, 441.

[36] Coriani, S.; Jørgensen, P.; Rizzo, A.; Ruud, K.; Olsen, J. *Chem. Phys. Lett.* **1999**, *300*, 61.

[37] Kjærgaard, T.; Jørgensen, P.; Thorvaldsen, A. J.; Sałek, P.; Coriani, S. *J. Chem. Theory Comput.* **2009**, *5*, 1997.

[38] Coriani, S.; Hättig, C.; Jørgensen, P.; Helgaker, T. *J. Chem. Phys.* **2000**, *113*, 3561.

[39] Seth, M.; Ziegler, T.; Banerjee, A.; Autschbach, J.; van Bisbergen, S. J. A.; Baerends, E. J. *J. Chem. Phys.* **2004**, *120*, 10942.

[40] Kristensen, K.; Kauczor, J.; Kjærgaard, T.; Jørgensen, P. *J. Chem. Phys.* **2009**, *131*, 044112.

[41] Norman, P.; Bishop, D. M.; Jensen, H. J. A.; Oddershede, J. *J. Chem. Phys.* **2001**, *115*, 10323.

[42] Ekström, U.; Norman, P. *Phys. Rev. A* **2006**, *74*, 042722.

[43] Cammi, R.; Mennucci, B. *J. Chem. Phys* **1999**, *110*, 9877.

[44] Cammi, R.; Frediani, L.; Mennucci, B.; Ruud, K. *J. Phys. Chem* **2003**, *119*, 5818.

[45] Lin, N.; Santoro, F.; Zhao, X.; Rizzo, A.; Barone, V. *J. Phys. Chem. A* **2008**, *112*, 12401.

[46] Herzberg, G.; Teller, E. *Z. Physik. Chem.* **1933**, *B12*, 410.

[47] Orlandi, G.; Siebrand, W. *J. Chem. Phys.* **1973**, *58*, 4513.

[48] Santoro, F.; Lami, A.; Improta, R.; Bloino, J.; Barone, V. *J. Chem. Phys.* **2008**, *128*, 224311.

[49] Mebel, A. M.; Chen, Y. T.; Lin, S. H. *J. Chem. Phys.* **1996**, *105*, 9007.

[50] Roos, B. O.; Malmquist, P. A.; Molina, V.; Serrano-Andrés, L. *J. Chem. Phys.* **2002**, *116*, 7526.

[51] Calaminici, P.; Köster, A. M.; Salahub, D. R. *J. Chem. Phys.* **2003**, *118*, 4913.

[52] Duschinsky, F. *Acta Physicochim.* **1937**, *7*, 551.

[53] Coutsias, E. A.; Seok, C.; Dill, K. A. *J. Comput. Chem.* **2004**, *25*, 1849.

[54] Sharp, T. E.; Rosenstock, H. M. *J. Chem. Phys.* **1964**, *41*, 3453.

[55] Doktorov, E. V.; Malkin, I. A.; Man'ko, V. I. *J. Mol. Spectrosc.* **1977**, *64*, 302.

[56] Santoro, F. *"FCclasses, a Fortran 77 code": visit http://villag.ipcf.cnr.it*.

[57] Santoro, F.; Improta, R.; Lami, A.; Bloino, J.; Barone, V. *J. Chem. Phys.* **2007**, *126*, 169903.

[58] Santoro, F.; Lami, A.; Improta, R.; Barone, V. *J. Chem. Phys.* **2007**, *126*, 184102.

[59] Santoro, F.; Barone, V. *Int. J. Quantum Chem.* **2009**, *110*, 476.

[60] Jankowiak, H.-C.; Stuber, J. L.; Berger, R. *J. Chem. Phys.* **2007**, *127*, 234101.

[61] Macak, P.; Luo, Y.; Ågren, H. *Chem. Phys. Lett.* **2000**, *330*, 447.

[62] Hazra, A.; Chang, H. H.; Nooijen, M. *J. Chem. Phys* **2004**, *121*, 2125.

[63] Heller, E. J. *J. Chem. Phys* **1978**, *68*, 3891.

[64] Heller, E. J. *Acc. Chem. Res.* **1981**, *14*, 368.

[65] Nooijen, M. *Int. J. Quantum Chem.* **2003**, *95*, 768.

[66] Neugebauer, J.; Baerends, E. J.; Nooijen, M. *J. Chem. Phys* **2004**, *121*, 6155.

[67] Cederbaum, L. S. *J. Chem. Phys.* **1983**, *78*, 5714.

[68] Nooijen, M. *Int. J. Quantum Chem.* **2006**, *106*, 2489.

[69] Lee, K.-M.; Yabana, K.; Bertsch, G. F. *J. Chem. Phys.* **2011**, *134*, 144106.

[70] Lanczos, J. *J. Res. Nat. Bur. Stand.* **1950**, *45*, 255.

[71] Nooijen, M.; Hazra, A. *VIBRON – A Program for Vibronic Coupling and Franck–Condon Calculations. With contributions from J. F. Stanton and K. Sattelmeyer*.

[72] Meier, A. R.; Wagnière, G. H. *Chem. Phys.* **1987**, *113*, 287.

[73] Gedanken, A.; Schnepp, O. *Chem. Phys.* **1976**, *12*, 341.

[74] Rizzo, A.; Coriani, S. *Adv. Quantum Chem.* **2005**, *50*, 143.

[75] Stich, T. R.; Brooks, A. J.; Buan, N. R.; Brunold, T. *J. Am. Chem. Soc.* **2003**, *125*, 5897.

Paper I

An IEF-PCM study of solvent effects on the Faraday B term of MCD

H. Solheim, L. Frediani, K. Ruud, and S. Coriani

Theor. Chem. Acc., **2008**, *119*, 231.

Paper II

Complex polarization propagator calculations of magnetic circular dichroism spectra

H. Solheim, K. Ruud, S. Coriani, and P. Norman
J. Chem. Phys., **2008**, *128*, 094103.

Paper III

The A and B terms of magnetic circular dichroism revisited

H. Solheim, K. Ruud, S. Coriani, and P. Norman
J. Phys. Chem A., **2008**, *112*, 9615.

Paper IV

Electronically excited states of Vitamin B_{12} and methylcobalamin: Theoretical analysis of absorption, CD and MCD data

H. Solheim, K. Kornobis, K. Ruud, and P. M. Kozlowski

J. Phys. Chem B., **2011**, *115*, 737.

Paper V

Vibrationally resolved circular dichroism spectra of a molecule with isotopically engendered chirality

N. Lin, H. Solheim, M. Nooijen, X. Zhao, K. Ruud, and M. Kwit

Manuscript.

Paper VI

On the systematic construction of vibronic coupling Hamiltonians: the interaction between the 1^1B_{3u} and 1^1B_{2u} states of pyrazine as an example

H. Solheim, A. Papp, C. Woywod, and K. Ruud

Manuscript.

ISBN xxx-xx-xxxx-xxx-x